Atmos. Chem. Phys. Discuss., 5, 11413–11487, 2005
www.atmos-chem-phys.org/acpd/5/11413/
SRef-ID: 1680-7375/acpd/2005-5-11413
European Geosciences Union

Atmospheric Chemistry and Physics Discussions

Conceptual study on nucleation burst evolution in the convective boundary layer – Part I: Modelling approach

O. Hellmuth

Modelling Department, Institute for Tropospheric Research, Permoser Str. 15, 04318 Leipzig, Germany

Received: 1 August 2005 – Accepted: 21 October 2005 – Published: 10 November 2005

Correspondence to: O. Hellmuth (olaf@tropos.de)

Abstract

A high-order modelling approach to interprete 'continental-type' particle formation bursts in the anthropogenically influenced convective boundary layer (CBL) is proposed. The model considers third-order closure for planetary boundary layer turbulence, sulfur and ammonia chemistry and aerosol dynamics. In part I of the present paper, previous observations of ultrafine particle evolution are reviewed, model equations are derived, the model setup for a conceptual study on binary and ternary homogeneous nucleation is defined, and shortcomings of process parameterization are discussed. In subsequent parts of the paper simulation results obtained within the framework of a conceptual study on the CBL evolution and new particle formation (NPF) will be presented and compared with observational findings.

1. Introduction

New particle formation (NPF) is known to widely and frequently occur in Earth's atmosphere (Kulmala et al., 2004, review). Among others, the question how multiscale transport processes influence NPF is not yet answered and subject of ongoing research. A review of scales and the potential of atmospheric mixing processes to enhance the binary nucleation rate was performed by Nilsson and Kulmala (1998). On the base of the classical concept of mixing-induced supersaturation – to our knowledge at first proposed by James Hutton in 1784 (Bohren and Albrecht, 1998, see p. 322–324) – Nilsson and Kulmala (1998) proposed a parameterization for the mixing-enhanced nucleation rate. The influence of atmospheric waves, such as Kelvin-Helmholtz instabilities on NPF was investigated by Bigg (1997), Nyeki et al. (1999), and Nilsson et al. (2000a). The effects of synoptic weather, planetary boundary layer (PBL) evolution, e.g., adiabatic cooling, turbulence, entrainment, and convection, respectively, on aerosol formation were analyzed in the marine boundary layer (MBL) (Russell et al., 1998; Pirjola et al., 2000; Coe et al., 2000; O'Dowd et al., 2002), in the continen-

ACPD

5, 11413–11487, 2005

tal boundary layer (CBL) (Nilsson et al., 2000b, 2001a,b; Aalto et al., 2001; Boy and Kulmala, 2002; Boy et al., 2004; Buzorius et al., 2001, 2003; Uhrner et al., 2003; Stratmann et al., 2003; Siebert et al., 2004), and in the free and upper troposphere (FT/UT) (Schröder and Ström, 1997; de Reus et al., 1999; Clarke et al., 1999; Khosrawi and Konopka, 2003; Hermann et al., 2003) as well. The influence of small-scale and sugrid-scale fluctuations, respectively, on the mean-state nucleation rate and the parameterization of turbulence-enhanced nucleation was subject of the investigation performed by Easter and Peters (1994), Lesniewski and Friedlander (1995), Andronache et al. (1997), Jaenisch et al. (1998a,b), Clement and Ford (1999b), Elperin et al. (2000), Hellmuth and Helmert (2002), Schröder et al. (2002), Buzorius et al. (2003), Housiadas et al. (2004), Shaw (2004) and Lauros et al. (2004).

Summing up previous works, further investigations are deserved to answer the following questions: (1) How strong can small-scale fluctuations enhance the nucleation rate during intensive mixing periods? (2) Can NPF be triggered by upward moving of air parcels across atmospheric layers with large temperature gradients? (3) Where does NPF occur in the PBL (within the surface layer or at levels above, followed by downward transport after breakup of the nocturnal residual layer and mixing of vapour and aerosol loaded surface layer with clean residual layer air)? Previous eddy covariance particle flux measurements above forests such as performed by, e.g., Buzorius et al. (2001, Figs. 4, 6, 8), Nilsson et al. (2001b, Fig. 9), and Held et al. (2004, Fig. 3) yield net deposition of particles, i.e., downward directed particles fluxes, but these measurements were restricted to altitudes nearby the canopy layer. To date, the net effect of forest stands on particle mass is not yet determined (Held et al., 2004).

Turbulence-related investigations of NPF are subject of ongoing research, e.g., on the European as well as on the process scale within the framework of the QUEST project (Quantification of Aerosol Nucleation in the European Boundary Layer, http://venda.uku.fi/quest/, http://www.itm.su.se/research/project.php?id=84).

Present day modelling studies to explain NPF events are often based on box models, e.g., applied within Lagrangian framework: (a) Analytical and semi-analytical burst

models, intended to be used for the parameterization of subgrid-scale (SGS) bursts in large scale global transport models (Clement and Ford, 1999a,b; Katoshevski et al., 1999; Clement et al., 2001; Dal Maso et al., 2002; Kerminen and Kulmala, 2002), (b) Multi-modal moment models (Kulmala et al., 1995; Whitby and McMurry, 1997; Wilck and Stratmann, 1997; Wilck, 1998; Pirjola and Kulmala, 1998), (c) Sectional models (Raes and Janssens, 1986; Kerminen and Wexler, 1997; Pirjola, 1999; Birmili et al., 2000; Korhonen et al., 2004; Gaydos and Stanier, 2005). Such models were demonstrated to succesfully describe NPF events when transport processes can be neglected. However, from in situ measurements Stratmann et al. (2003) and Siebert et al. (2004) provided evidences for a direct link between turbulence intensity near the CBL inversion and ground-observed NPF bursts on event days. When, e.g., CBL turbulence is suspected to be important, occurrence and evolution of NPF bursts are not yet satisfying modelled (Birmili et al., 2003; Wehner and Wiedensohler, 2003; Stratmann et al., 2003; Uhrner et al., 2003). Independent from the degree of sophistication, zero-dimensional models are a priori not able to explicitely descibe transport processes, neither grid-scale nor SGS ones. At most, such models can implicitely consider transport effects by more or less sophisticated artificial tendency terms (e.g., for entrainment) or by empirically adjusted tuning parameters. For example, Uhrner et al. (2003, Figs. 1 and 5) derived a semi-empirically prefactor for the binary nucleation rate to correct for the influence of vertical exchange processes in their box model study. The logarithm of that pre-factor varied from −3 to 17.2 depending on the local temperature gradient in the Prandtl layer, whereas largest values were obtained for very unstable conditions.

To overcome present shortcomings in NPF burst modelling, Boy et al. (2003) proposed a one-dimensional boundary layer model with aerosol dynamics and a second-order turbulence closure (BLMARC) including binary and ternary nucleation. The underlying assumption of horizontal homogeneinity is justified by the fact that NPF often quasi-simultaneously occurs over distances ranging from approximately 50 km to the synoptic scale with a horizontal extension of more than 1000 km (Nilsson et al., 2001a; Birmili et al., 2003; Stratmann et al., 2003; Wehner et al., 2003; Plauskaite et al., 2003;

Komppula et al., 2003; Vana et al., 2004; Gaydos and Stanier, 2005).

As a contribution to the ongoing discussion on the role of turbulence during the evolution of 'continental-type' NPF bursts in anthropogenically influenced regions, a columnar modelling approach is proposed here. Compared to former studies, CBL dynamics, chemistry reactions and aerosol dynamics will be treated in a self-consistently manner by applying higher-order closure to PBL dynamics, appropriate sulfur and ammonia chemistry and aerosol dynamics.

A comprehensive explanation of the annotation applied in turbulence closure techniques can be found, e.g., in Stull (1997, Chapter 6, p. 197–250). In general, the closure problem is a direct consequence of Reynolds' flow decomposition and averaging approach (Stull, 1997, p. 33–42). The closure problem results from the fact, that *"the number of unknowns in the set of equations for turbulent flow is larger than the number of equations"* (Stull, 1997, p. 197). The introduction of additional diagnostic or prognostic equations to determine these unknown variables results in the appearance of even more new unknowns. Consequently, the total statistical description of a turbulent flow requires an infinite set of equations. In opposite to this, for a finite set of gouverning equations the description of turbulence is not closed. This fact is commonly known as the *"closure problem"*. As demonstrated by Stull (1997, Tables 6–1, p. 198), the prognostic equation for any mean variable $\overline{\alpha}$ (first statistical moment) includes at least one double correlation term $\overline{\alpha'\beta'}$ (second statistical moment). The forecast equation for this second-moment turbulence term contains additional triple correlations terms $\overline{\alpha'\beta'\gamma'}$ (third statistical moments). Subsequently, the gouverning equations for the triple correlations contain fourth-moment quantities $\overline{\alpha'\beta'\gamma'\delta'}$, yadda-yadda-yadda. For practical reasons only a finite number of equations can be solved, and the remaining unknowns have to be parameterized in terms of known variables: *"Such closure approximations or closure assumptions are named by the highest order prognostic equations that are retained"* (Stull, 1997, p. 199). For example, in a first-order closure scheme only first-moment variables are predictive, and second-order moments are parameterized. In a second-order closure scheme first-moment and second-moment variables are pre-

dictive, and third-moment variables are parameterized. Finally, in a third-order closure scheme all first-moment, second-moment, and third-moment variables are determined via prognostic equations, while the fourth-moment variables are parameterized in terms of lower-moment variables. With respect to the treatment of the *"parameterization problem"* the reader is referred as well to Stull's ostensive perception of this tricky subject, which culminates in a quotation of Donaldson (1973): *"There are more models for closure of the equations of the motion at the second-order correlation level than there are principal investigators working on the problem"* (Stull, 1997, p. 201). Considering the important role of human interpretation and creativity in the construction of approximations, the parameterization can be to some degree located at an intermediate stage between science and art. Hence, *"parameterization will rarely be perfect. The hope is that it will be adequate"* (Stull, 1997, p. 201).

So far, previous attempts to extend third-order closure to aerosol dynamics in the PBL are not known. In this paper, the approach is motivated, model formalism and assumptions are described. In subsequent papers, a conceptual study on meteorological and physico-chemical conditions that favour NPF in the anthropogenically influenced CBL will be performed.

2. Characterization of 'continental-type' new particle formation bursts

In each case over a period of 1.5 years, Birmili and Wiedensohler (2000) observed NPF events in the CBL on approximately 20% of all days, Stanier et al. (2003, Pittsburgh region, Pennsylvania) on over 30% of the days, most frequent in fall and spring, and least frequent in winter. NPF was observed to be favoured on sunny days with below average $PM_{2.5}$ concentrations. NPF events were found to be fairly correlated with the product of UV intensity and sulfur dioxide concentration, and to be dependent on the effective area available for condensation, indicating that sulfuric acid is a component of new particles. Held et al. (2004, BEWA field campaign in summer 2001 and 2002) observed NPF on approximately 22% of all days at a ecosystem research site

in the Fichtelgebirge mountains, Bavaria. During a 15 month field campaign Gaydos and Stanier (2005, Pittsburgh Air Quality Study (PAQS)) observed regional NPF on approximately 33% of all days. In general, NPF events are characterized by a strong increase in the concentration of nucleation mode particles (diameter <10 nm, particle number concentration $>10^4\,cm^{-3}$), a subsequent shift in the mean size of the nucleated particles, and the gradual dissapearence of particles over several hours (Birmili and Wiedensohler, 2000; Birmili, 2001). Figure 1 shows a generalized pattern of the diurnal evolution of the number concentration of ultrafine concentration nuclei (UCN) during a typical NPF event observed in the convective surface layer (CSL). The typical UCN evolution shown in that figure is derived from a number of previous observations, e.g., published by Clement and Ford (1999a, Fig. 2), Coe et al. (2000, Fig. 1), Birmili and Wiedensohler (2000, Fig. 1), Birmili et al. (2000, Figs. 1 and 2), Kulmala et al. (2001, Fig. 1), Nilsson et al. (2001a, Fig. 4), Aalto et al. (2001, Figs. 8, 11, 13), Buzorius et al. (2001, Fig. 6), Clement et al. (2001, Fig. 1), Boy and Kulmala (2002, Fig. 1), Boy et al. (2004, Figs. 1 and 2), Boy et al. (2003c, Fig. 1), Birmili et al. (2003, Figs. 1, 2, 4, 5, 14), Buzorius et al. (2003, Fig. 6), Stratmann et al. (2003, Figs. 10, 11, and 17), Siebert et al. (2004, Fig. 3), Steinbrecher et al. (2004, Fig. 5), O'Dowd et al. (2004, Fig. 3), Kulmala et al. (2004, Fig. 2), Held et al. (2004, Figs. 1, 2, 3), Gaydos and Stanier (2005, Figs. 1, 3, 4).

The aim of the present approach is twofold: (a) to reproduce the typical UCN evolution during a NPF event as represented in Fig. 1, (b) to propose a suitable method for the estimation of chemical composition fluxes of the particulate phase, e.g., suggested to be a major task for future PBL research (Held et al., 2004).

3. Modelling approach

3.1. Rationale of non-local and high-order modelling

The modelling approach is motivated by the following facts: (1) Local closure (known, e.g., as K-, small-eddy, or downgradient theory) is generally accepted to be only valid if the characteristic scale of turbulent motions is very small compared to the scale of the mean flow as given for stable and neutral conditions. (2) During convective conditions, the dominant eddy length scale often exceeds the CBL depth, hence (2.1) turbulent motions are not completely SGS in grid layers, (2.2) vertical gradients in the well-mixed layer are usually very weak, (2.3) entrainment fluxes can significantly alter the CBL dynamics, and (2.4) countergradient transports can take place in nearly the entire upper part of the CBL (Sorbjan, 1996; Sullivan et al., 1998). Countergradient transports are relevant for turbulent heat, momentum and concentration fluxes (Holtslag and Moeng, 1991; Frech and Mahrt, 1995; Brown, 1996; Brown and Grant, 1997). Consequently, for unstable conditions non-local closure techniques are required even for horizontally homogeneous turbulence over flat surface and zero mean wind (Ebert et al., 1989; Pleim and Chang, 1992). Nevertheless, even most of state-of-the-art non-local mixing schemes have difficulties to represent the entrainment processes at the top of even the clear boundary layer (Ayotte et al., 1996; Siebesma and Holtslag, 1996; Abdella and McFarlane, 1997, 1999; Mironov et al., 1999). (3) Turbulent non-local transport was demonstrated to be important not only in convective turbulence but also in neutral conditions, hence deserving to be accounted for in PBL modelling (Ferrero and Racca, 2004). (4) As gradients of chemical concentrations are often more severe than gradients of heat, moisture, and momentum non-local closure is much more stringent for atmospheric chemistry models than for meteorological ones (Pleim and Chang, 1992). In addition, in the CBL reactants were found to be normally segregated. Under such conditions, chemical transformations depend on turbulent mixing, especially when the time-scale of the chemical transformations is in the order of the turbulent characteristic time scale. Then, the mean transformation rate of multimolecular reactions can

be strongly affected by covariances of concentration fluctuations, which deserves, e.g., an adjustment of the eddy diffusivity or parameterization of effective reaction rates accounting for inefficient mixing due to subgrid-scale turbulence in terms of large-scale grid length (Galmarini et al., 1997; Verver et al., 1997; Thuburn and Tan, 1997; Vinuesa and Vilá-Guerau de Arellano, 2005). Thuburn and Tan (1997, see references therein) demonstrated that the neglection of covariance terms in chemical reaction rates can cause significant errors in predicted chemical rates. Vinuesa and Vilá-Guerau de Arellano (2005) demonstrated that heterogeneous mixing due to convective turbulence importantly impacts chemical transformations by slowing down or increasing the reaction rate depending on whether reactants are transportes in opposite direction or not. (5) Higher-order closure becomes more and more common in modelling physical climate processes and their feedbacks (IPCC, 2001, Sect. 7.2.2.3). A comprehensive review and discussion of state-of-the-art parameterizations of triple correlations and SGS condensation can be found in Zilitinkevich et al. (1999) and Abdella and McFarlane (2001). Recent high-order modelling studies were performed, e.g., by Cheng et al. (2004), Ferrero and Racca (2004), Larson (2004), Lewellen and Lewellen (2004), and Vinuesa and Vilá-Guerau de Arellano (2005).

3.2. Model description

The closure approach adapted here, inclusive approximations (e.g., Rotta's return-to-isotropy hypothesis for pressure covariance terms, quasi-normal approximation for the quadruple correlations, clipping approximation for ad hoc damping of excessive growing triple correlations), parameterization of turbulence-length scale, numerical model (discretization, integration scheme, filtering of spurious oscillations), initial- and boundary conditions as well as stability analysis are based on the third-order modelling studies of André et al. (1976a,b, 1978, 1981) as well as on second-order ones of Wichmann and Schaller (1985, 1986), Verver et al. (1997) for the cloudless PBL.

To ensure traceability, the final equations are given in the Appendix, whereas Appendix B contains the non-filtered model, Appendix C the filtered one.

3.2.1. PBL model

The PBL model includes predictive equations for the horizontal wind components, the potential temperature, and the water vapour mixing ratio (Appendix B1).

To calculate the surface fluxes of momentum, heat and humidity a semi-empirical flux separation scheme proposed by Holtslag (1987) is used. It solves the surface energy budget by a simplified Penman-Monteith approach.

The diabatic heating/ cooling rate due to longwave and shortwave radiation, i.e., $(\partial\overline{\theta}/\partial t)_{\mathrm{rad}}=\overline{\theta}/\overline{T})\times(\partial\overline{T}/\partial t)_{\mathrm{rad}}$, is calculated according to Krishnamurti and Bounoua (1996, p. 194–207). For the longwave radiation an emissivity tabulation method is used. In this method, the emissivity is expressed as a function of the path length which in turn depends on temperature, pressure, and relative humidity. The basic emissivity values are given in a look-up-table, from which the actual value of emissivity is then interpolated for given path length. Only absorption and emission by water vapour is considered. The calculation of shortwave radiation is based on an empirical absorptivity function of water vapour. Aerosols are not considered in the radiation model. The radiative transfer calculations are performed at each time step.

Vertical advection due to large-scale subsidence is considered by an empirically prescribed subsidence velocity. For fair weather conditions, anticyclones etc., associated with clear skies and strong nocturnal radiative cooling Carlson and Stull (1986) found vertical velocities of $-0.1 \ldots -0.5\,\mathrm{m\,s^{-1}}$ near the top of the stable boundary layer.

As a consequence of the quasi-normal approximation etc., the third-order moment equations were demonstrated to be of hyperpolic type ("wave equation") containing non-physical solutions called "spurious oscillations" (Moeng and Randall, 1984). Wichmann and Schaller (1985) argued that spurious oscillation solutions are neither typical for nor restricted to third-order closure models, and arise from the use of explicite time-differencing scheme. Using a second-order scheme, the authors showed that spurious oscillations can be suppressed by use of an implicit time-differencing scheme. In the present version, an explicit time-differencing scheme is retained. To damp spurious os-

ACPD
5, 11413–11487, 2005

cillations, an artificial diffusion term is added to the right-hand sides of the third-order moment equations as recommended by Moeng and Randall (1984).

3.2.2. Chemical model

The chemical model consists of three predictive equations for NH_3, SO_2, and H_2SO_4 which consider emission, gas-phase oxidation, heterogeneous nucleation (condensation loss on nucleation, Aitken and accumulation mode particles), molecule loss due to homogeneous nucleation, and dry deposition (Appendix B2). To reduce the chemical mechanism, the OH evolution is diagnostically prescribed.

3.2.3. Aerosol model

The aerosol model is based on a monodisperse approach proposed by Kulmala et al. (1995), Pirjola and Kulmala (1998), and Pirjola et al. (1999, 2003). It consists of predictive equations for two moments (number and mass concentration) in three modes (nucleation, Aitken, accumulation mode), and considers homogeneous nucleation, heterogenous nucleation (condensation onto the particles surfaces), intra- and intermode coagulation, and dry particle deposition (Appendix B3).

3.2.4. Nucleation model

The calculation of the nucleation rate is based on the classical theory of homogeneous nucleation. Thereafter, the rate of homogeneous nucleation J, i.e., the number of newly formed critical "embryo's", or nuclei per volume and time unit, is a product of a kinetic and thermodynamical part, $J{=}K\exp(-G_{sp}/(kT))$. The prefactor K is mainly based on nucleation kinetics, and the thermodynamical part is proportional to the Gibbs free energy of the critical cluster G_{sp} (Kulmala et al., 2003). Owing to limited solvation, small clusters are less stable then the bulk, which leads for moderate supersaturation to the formation of a barrier on the Gibbs free energy surface for cluster growth (Lovejoy et al., 2004). Nucleation according to classical theory is limited by barrierless nucleation

where the formation energy is zero and only kinetic contribution is included. The kinetic part itself is smaller the lower vapour concentration is (Kulmala et al., 2003).

Corresponding to the number of participating species, the validity of binary and ternary classical nucleation theory are subject of controverse discussions.

Binary nucleation theory is known for their large uncertainties in explaining observed nucleation rates. The difference between predicted and observed nucleation rates can exceed several orders of magnitude (Pandis et al., 1995; Kulmala et al., 1998). NPF often occurs at H_2SO_4 concentrations lower and observed nucleation frequencies are often higher than that predicted by classical binary nucleation theory, the detailed chemistry of the events remains uncertain (de Reus et al., 1998; Stanier et al., 2003). On the other side, binary nucleation is supported by the fact that many observed NPF events are associated with elevated SO_2 levels and photochemically induced production of H_2SO_4 vapour (e.g. Marti et al., 1997) as well as by the dominating contribution of sulphate to the total aerosol mass as, e.g., shown by Müller (1999) for a rural continental test site influenced by power plants. Strong arguments for kinetically-controlled binary nucleation were provided by Weber et al. (1996) and Yu (2003). The nucleation rate can be enhanced due to the higher stability of embryonal H_2O/H_2SO_4 clusters, which increases the cluster lifetime and hence, the chance of such a cluster to grow into a particle of detectable size (de Reus et al., 1998).

Compared to binary nucleation theory, ternary one of $H_2O/H_2SO_4/NH_3$ predicts significantly higher nucleation rates and more frequent nucleation under typical tropospheric concentrations of H_2SO_4 and NH_3 (Korhonen et al., 1999). This is due to the effect that NH_3 is able to stabilize the critical embryo, i.e., to reduce its size leading to enhanced nucleation rates (Yu, 2003; Weber et al., 1996).

Recently, Berndt et al. (2005) performed laboratory experiments on NPF, in which an atmospheric pressure flow-tube was irradiated with ultraviolet light to produce H_2SO_4 in situ through reaction of OH with SO_2. Newly formed particles were observed for H_2SO_4 concentrations above 7×10^6 cm^{-3}. For a temperature of 293 K, relative humidities ranging from 28–49.5% and NH_3 concentrations below 0.5 pptv, the authors ob-

served a nucleation rate of 0.3–0.4 cm^{-3} s^{-1} for a H_2SO_4 concentration of $\sim 10^7$ cm^{-3} (particle size $\geq$3 nm). This nucleation rate was found to be inline with the lower limit of the nucleation rates observed in the atmosphere. Because of the very low NH_3 concentration of $\leq$0.5 pptv in the flow tube compared to 100 to 10 000 pptv in the continental boundary layer, the authors called the substantial role of NH_3 in the nucleation process into question. ¿From a comparison of the experimental nucleation rates with theoretical ones of Vehkamäki et al. (2002) and Napari et al. (2002a) the authors concluded that the H_2SO_4 concentration required for substantial binary nucleation is $\sim 10^{10}$ cm^{-3}, i.e., which is far above the experimental values. In view of the very low NH_3 concentration, its influence onto nucleation was excluded. Hence, currently available binary nucleation theories, ion-induced nucleation, as well ternary NH_3-influenced nucleation were excluded from explaining observed NPF. The power law dependency of nucleation rate on H_2SO_4 concentration, obtained by Berndt et al. (2005), is very similar to a kinetically controlled nucleation mechanism.

Apart from the question, which species contribute to nucleation, classical nucleation theory suffers from two essential shortcomings: (1) Molecular clusters are represented by "droplets" up to and including the critical size, characterized by bulk properties of the condensed phase, such as surface tension, density, vapour pressure (Yu and Turco, 2001). This so-called "capillarity approximation" is known to be inappropriate for small molecular clusters with $\sim$1 nm diameter and causes large uncertainties in nucleations rates predicted by classical theory (Lovejoy et al., 2004). (2) According to the classical theory, NPF performs instantaneously, i.e., the time scale of the growth kinetics of the subcritical embryos is neglected compared to other relevant time scales in aerosol evolution (Yu and Turco, 2001).

To overcome these shortcomings in general, self-consistent kinetic theory is desired. In the kinetic theory, the cluster formation is described as a sequence of basic collision steps beginning with the vapour phase (Yu and Turco, 2001). Afterwards, molecular scale coagulation and dissociation act as the driving processes of aerosol evolution. Condensation and coagulation are treated analogeously, i.e., condensation (evapora-

tion) is equivalent to coagulation (dissociation) of a molecule or small molecular cluster with (from) a particle (Yu and Turco, 2001). Kinetic theory can explicitely describe interacting systems of vapours, ions, charged and neutral clusters, and preexisting aerosols at all sizes in a straightforward and self-consistent manner. Being physically more realistic and flexible it is considered to be superior to the classical approach (Yu and Turco, 2001).

However, compared to new theoretical approaches based on, e.g., ab initio molecular dynamics and Monte Carlo simulations, the classical nucleation theory is still the only one which can be used in atmospheric modelling, even if molecular approaches are needed to confirm results obtained by classical theories (Noppel et al., 2002). At least, the time scale of the growth kinetics of the subcritical embryos can be a posteriori considered in classical theory by adapting the concept of "apparent nucleation rate" (Kerminen and Kulmala, 2002). The apparent nucleation rate is the rate at which newly formed particles with detectable size appear in the sensor detection range. When new embryo's, i.e., "critical clusters" with ~1 nm diameter, grow in size by condensation and intra-mode coagulation, their number concentration decreases. As a result, the apparent nucleation rate is lower than the real one derived from nucleation theory. Kerminen and Kulmala (2002) derived an analytical formula to relate the apparent to the real nucleation rate for application in explicit nucleation schemes in atmospheric models to cut-off the lowest desirable scale for the evolution of the aerosol size distribution. However, this formula is not applicable to very intensive nucleation bursts, to potential nucleation events associated with cloud outflows, or to nucleation occuring in plumes undergoing strong mixing with ambient air.

In the present approach, for calculation of the homogeneous binary H_2O/H_2SO_4 nucleation rate and critical cluster composition the so-called "exact" model with consideration of cluster hydration effects is implemented (Stauffer, 1976; Jaecker-Voirol et al., 1987; Jaecker-Voirol and Mirabel, 1988, 1989; Kulmala and Laaksonen, 1990; Laaksonen and Kulmala, 1991; Kulmala et al., 1998; Seinfeld and Pandis, 1998). For the ternary $H_2O/H_2SO_4/NH_3$ nucleation rate and critical cluster composition a

state-of-the-art parameterization is used (Napari et al., 2002a,b). The limits of the validity of the ternary nucleation parameterization are T=240–300 K, RH=5–90%, $[H_2SO_4]=10^4-10^9$ molecules cm^{-3}, $[NH_3]$=0.1–100 ppt, and $J_{ter}=10^{-5}-10^6$ cm^{-3} s^{-1}. The parameterization cannot be used to obtain the binary H_2O/H_2SO_4 or H_2O/NH_3 limit (Napari et al., 2002b). When the vapour concentrations fall below their lower parameterization limits they were kept at their correspondig minimum concentrations.

3.2.5. Condensation flux model

The condensation flux represents the vapour molecular deposition rate onto spherical droplets of a certain radius. It results from mass transfer solution of the transport equation in the continuum regime, i.e., when the particle is sufficiently large compared to the mean free path of the diffusing vapour molecules. The solution obtained by Maxwell (1877) describes the total flow of vapour molecules toward an aerosol particle by diffusion on a molecular scale (Seinfeld and Pandis, 1998, p. 596–597, Maxwellian flux). When the mean free path length of diffusing vapour becomes comparable to the particle diameter, the Maxwellian flux needs to be corrected by the so-called Fuchs-Sutugin factor in terms of Knudsen number. The correction factor extends the growth rate from the contiuum regime into the transition regime. In the present approach, the condensation flux parameterization is applied to nucleation, Aitken and accumulation mode particle. The Maxwellian flux is proportional to the driving force, i.e., the difference between the partial pressure of the condensable vapour far from the particle (ambient conditions) and the vapour pressure at the droplet surface, the latter being a product of equilibrium partial pressure at ambient temperature and the acid activity in the condensed phase. If the driving force is positive, the flow of vapour molecules is directed toward the particle, and if negative vice versa. In the present approach, maximum Maxwellian flux is considered, i.e., the ratio of the vapour pressure at the droplet surface to the ambient partial pressure is assumed to be much lower than 1, which means that the diffusive flux is always directed to the particle surface.

This assumption is widely accepted to be valid for low-volatile vapours such as sul-

furic acid (Seinfeld and Pandis, 1998; Clement and Ford, 1999a,b; Liu et al., 2001; Krejci et al., 2003; Boy et al., 2003c; Held et al., 2004; Gaydos and Stanier, 2005), and for organic molecules such as dicarboxylic acids and for pinon aldehyde as the main product of α-pinene oxidation (Boy et al., 2003c; Held et al., 2004).

However, with respect to atmospheric NH_3 the assumption of maximum Maxwellian flux is questionable. As demonstrated by Nenes et al. (2000), the vapour pressure at the droplet surface strongly depends, e.g., on droplet composition. In their NPF modelling study, Gaydos and Stanier (2005) argued that H_2SO_4 condensation alone produces growth that is similar to observations, hence NH_3 condensation by molecular diffusion was not considered explicitely. Instead, NH_3 gas phase concentration was diagnostically determined from the assumption, that total ammonia, total nitrate and sulfate, taken from measurements, are always in thermodynamic equilibrium with gas and particulate phase concentrations (Ansari and Pandis, 1999, model GFEMN). Here, a similar approach is applied. The gas phase NH_3 concentration is diagnostically determined for given total ammonium and sulfate concentration (gas + aerosol phase), using the inorganic aerosol thermodynamic equilibrium model ISORROPIA (meaning "equilibrium" in Greek) of Nenes et al. (2000), whereas total ammonium and sulfate concentration are prognostically determined.

3.2.6. Humidity growth

The water uptake of dry aerosol is considered by applying the empirical humidity growth factor of Birmili and Wiedensohler (2004, pers. communication).

3.2.7. Particle deposition model

The size-segregated particle dry deposition velocity is parameterized according to Zhang et al. (2001).

4. Conclusions

Based on previous findings on high-order modelling an attempt is made to describe gas-aerosol-turbulence interactions in the CBL. The approach can be characterized as follows:

1. A third-order closure is self-consistently applied to a system of meteorological, chemical and quasi-linearized aerosol-dynamical equations under horizontally homogeneous conditions.

2. The model is designed to predict time-height profiles of meteorological, chemical, and aerosol-dynamical mean-state variables, variances, co-variances and triple correlations in the CBL.

3. The approach might be instrumental in interpreting observed particle fluxes from in situ measurements and/or remote sensing. In addition, it provides information about gas-aerosol-turbulence interactions that cannot be directly observed in the CBL.

4. Though highly parameterized, the model configuration considers the pimary processes supposed to be involved in the evolution of NPF bursts in the CBL.

5. The model provides input information required for a more sophisticated parameterization of the effect of subgrid-scale turbulence on the homogeneous nucleation rate, such as variances and co-variances of temperatures, humitity, and the condensable vapours sulfuric acid and ammonia (Easter and Peters, 1994; Hellmuth and Helmert, 2002; Shaw, 2004; Lauros et al., 2004).

6. Provided that the model is validated, it may serve as a tool, e.g., to perform conceptual studies and to verify parameterizations of SGS processes in large-scale chemistry and aerosol models (effective reaction rates, turbulence-enhanced condensation etc.).

Known shortcomings of the nucleation approach and condensation flux parameterization are discussed. To consider turbulent density fluctuations the gouverning equations for the first-, second- and third-order moments must be re-derived on the base of a scale analysis (Bernhardt, 1964, 1972; Bernhardt and Piazena, 1988; Foken, 1989; Venkatram, 1993; van Dop, 1998). Part II to IV of the paper demonstrate the model capability to predict CBL evolution in terms of first-, second- and third-order moments, and to simulate the UCN evolution during a NPF event within the framework of a conceptual study. Furthermore, the model results are interpreted with respect to previous observational findings.

Appendix A

List of symbols, annotations, scaling properties, constants, parameters, and abbreviations

A1. Symbols

a_1, a_2 – Empirical parameters for the incoming solar radiation
$\alpha_{H_2SO_4}$ – Accomodation coefficient of sulfuric acid vapour
α_T – Coefficient of thermal expansion
$\alpha_0 = 1/\mathrm{Pr_t}$ – Reziproke of turbulent Prandtl number
α_{sfc} – Albedo of the surface
α_{PM} – Empirical parameter for Penman–Monteith approach
b_1, b_2 – Empirical parameters for the incoming solar radiation
$\beta_{buo} = \alpha_T \times g$ – Buoyancy parameter
β_{PM} – Empirical parameter for Penman–Monteith approach
$C_1, \ldots, C_{11}$ – Adjustment parameters for the turbulence closure scheme
C_{coag} – Brownian coagulation coefficient [$m^3 s^{-1}$]
$C_{cond,gas}$ – Condensation coefficient [$m^3 s^{-1}$]
$c_1, \ldots, c_3$ – Empirical parameters for the surface energy budget
c_G – Empirical parameter for the soil heat flux
χ_α – Reactive tracer and/or aerosol parameter $\{\alpha = 1, \ldots, N\}$
$D_{H_2SO_4}$ – Diffusion coefficient of sulfuric acid vapour
D_i – Stokes–Einstein like expression for the diffusion coefficient
D_{pi} – Particle diameter
e – Turbulent kinetic energy
ε – Dissipation rate
ε_R – Radiative destruction rate
$\mathcal{F}$ – Modified Fuchs–Sutugin factor

ACPD
5, 11413–11487, 2005

f_c – Coriolis parameter
Φ_{sun} – Solar elevation
ϕ – Geographical latitude
ϕ_m, ϕ_h – Similarity function for momentum and heat
G_{soil} – Soil heat flux
g – Acceleration of gravity
Γ_d – Dry adiabatic lapse rate
γ – Psychrometric constant
GF – Growth factor
H_{sfc} – Sensible heat flux at the surface
H_{χ_α} – χ_α scale heigt $\{\alpha = 1, \ldots, N\}$
H_w – Scale heigt of large – scale subsidence
J_{nuc} – Nucleation rate [$\text{m}^{-3}\text{s}^{-1}$]
$K^{\downarrow}$ – Incoming solar radiation at ground level
$K^{\downarrow}_{\text{clear}}$ – Incoming solar radiation at ground level in clear skies
Kn – Knudsen number
$\mathcal{K}^{\alpha} = (k^{\alpha}_{mn})$ – "Coupling matrix", i.e., reaction rates between tracer χ_{m} and χ_{n} in reaction equation α $\{(m, n) = 1, \ldots, N, \alpha = 1, \ldots, N\}$
K_m, K_h – Eddy diffusion coefficients for momentum and heat
k_1 – Pseudo–second order rate coefficient for the reaction of OH with H_2SO_4
L – Monin–Obukhov length scale
L_{turb} – Turbulence–length scale
$L_{\text{Blackadar}}$ – Blackadar's length–scale for neutral and unstable stratification
L_D – Turbulence–length scale for stable stratification
$L^{\downarrow}$ – Incoming longwave radiation from the atmosphere
$L^{\uparrow}$ – Outgoing longwave radiation from the surface
L_v – Latent heat of water vapourization

ACPD
5, 11413–11487, 2005

$L_v E_{sfc}$ – Latent heat flux
λ_{air} – Air mean free path
M_i – Mode i particle mass concentration [kg m^{-3}] $\{i = 1, \ldots, 3\}$
m_i – Mode i mean dry particle mass [kg] $\{i = 1, \ldots, 3\}$
$m_{H_2SO_4}$ – Mass of one H_2SO_4 molecule [kg]
μ_{air} – Viscosity of air
N_{cld} – Total cloud cover
N_i – Mode i particle number concentration [m^{-3}] $\{i = 1, \ldots, 3\}$
$n^*_{NH_3}$, $n^*_{H_2SO_4}$ – Number of NH_3 and H_2SO_4 molecules per newly formed embryo
n_{OH} – Exponent in OH representation
n_w – Exponent in representation of large – scale subsidence
$[OH]_{min}$, $[OH]_{max}$ – Minimum and maximum OH concentration
ω – Angular velocity of the earth
P – Generation rates of eddy kinetic energy $\overline{e}$
P_{ij} – Generation rates of Reynolds stresses $\overline{u'_i u'_j}$
P_{ia} – Generation rates of scalar flux $\overline{u'_i a'}$
P_{relax}, P_{rapid} – Relaxation and rapid part of pressure triple term
$\mathrm{Pr_t} = \frac{K_m(\zeta = 0)}{K_h(\zeta = 0)}$ – Turbulent Prandtl number
Ψ_M, Ψ_H – Stability functions for momentum and heat
Q^* – Net radiation at the surface
Q_α – Source term in the gouverning equation of reactant α $\{\alpha = 1, \ldots, N\}$
$Q_{\alpha,emission}$ – Emissions of reactant α $\{\alpha = 1, \ldots, N\}$
q – Water vapour mixing ratio
q_* – Kinematic humidity scale
R_α – Reaction/interaction term in the gouverning equation of tracer α $\{\alpha = 1, \ldots, N\}$
RH – Relative humidity

$r_{i,\mathrm{dry}}$, $r_{i,\mathrm{wet}}$ – Mode i mean radius of the dry and wet aerosol [m] $\{i = 1, \ldots, 3\}$
ρ_p – Particle density
σ – Stefan–Boltzmann constant
T – Temperature
T_{scr} – Temperature at screening height (1–2 m)
θ – Potential temperature
$\theta_\star$ – Kinematic temperature scale
$(\partial\theta/\partial t)_{\mathrm{rad}}$ – Diabatic heating/cooling rate due to radiative flux divergency
u_i, u_j – Components of three–dimensional wind vector $\{(i, j) = 1, \ldots, 3\}$
u – x–component of horizontal wind
u_g – x–component of geostrophic wind
$u_\star$ – Friction velocity
U – Horizontal wind velocity
v – y–component of horizontal wind
v_g – y–component of geostrophic wind
V_{χ_α} – Deposition velocity $\{\alpha = 1, \ldots, N\}$
w – Large–scale subsidence velocity
w_H – Large–scale subsidence velocity at H_w
$w_\star$ – Convective velocity scale
z_0 – Surface roughness length
z_s – Height level just above the surface (screening height)
$z_p = z_{\mathrm{k=1}}$ – Prandt layer height (first main level)
z_i – Mixing layer height
$\zeta = z/L$ – Dimensionless height

ACPD
5, 11413–11487, 2005

A2. Constants

$a_1 = 1041\,\mathrm{W\,m^{-2}}$
$a_2 = -69\,\mathrm{W\,m^{-2}}$
$\alpha_{H_2SO_4} = 0.12$
$\alpha_T = 1/T_0 = 3.51 \times 10^{-4}\,\mathrm{K^{-1}}$
$\alpha_{PM} = 1$
$\alpha_{sfc} = 0.23$
$b_1 = 0.75$
$b_2 = 3.4$
$\beta_{PM} = 20\,\mathrm{W\,m^{-2}}$
$C_2 = 2.5$
$C_4 = 4.5$
$C_5 = 0$
$C_6 = 4.85$
$C_7 = 0.4$
$C_8 = 8.0$
$C_{10} = 6.0$
$C_{11} = 0.2$
$c_1 = 5.31 \times 10^{-13}\,\mathrm{W\,m^{-2}\,K^{-6}}$
$c_2 = 60\,\mathrm{W\,m^{-2}}$
$c_3 = 0.12$
$c_g = 0.1$
$c_h = \alpha_0\,\kappa$
$c_m = \kappa$
$c_{pa} = 1006\,\mathrm{J\,kg^{-1}\,K^{-1}}$
$D_{H_2SO_4} = 1.2 \times 10^{-5}\,\mathrm{m^2\,s^{-1}}$
$\eta_1 = 0.097$

ACPD
5, 11413–11487, 2005

$\eta_2 = 0.204$

$\eta_3 = 5.5826$

$f_c = 2\omega \sin\phi \approx 1.117 \times 10^{-4}\,\mathrm{s}^{-1}$

$g = 9.80665\,\mathrm{m}^2\,\mathrm{s}^{-1}$

$\gamma = c_p/L_{v,0} \approx 4 \times 10^{-4}\,\frac{q_{\mathrm{water}}}{q_{\mathrm{air}}}\mathrm{K}^{-1}$

$\Gamma_d = g/c_p \approx 1\,\mathrm{K}/100\,\mathrm{m}$

$k_1 = 1.5 \times 10^{-18}\,\mathrm{m}^3\,\mathrm{molecules}^{-1}\,\mathrm{s}^{-1}$

$k_B = 1.381 \times 10^{-23}\,\mathrm{J\,K}^{-1}$

$\kappa = 0.41$

$L_{v,0} = 2515 \times 10^3\,\mathrm{J\,kg}^{-1}$

$\lambda_{\mathrm{air}} = 6.98 \times 10^{-8}\,\mathrm{m}$

$M_{\mathrm{SO}_2} = 64.06 \times 10^{-3}\,\mathrm{kg\,mol}^{-1}$

$M_{\mathrm{NH}_3} = 17.0318 \times 10^{-3}\,\mathrm{kg\,mol}^{-1}$

$M_{\mathrm{H_2SO_4}} = 98.08 \times 10^{-3}\,\mathrm{kg\,mol}^{-1}$

$\mu_{\mathrm{air}} = 1.83 \times 10^{-5}\,\mathrm{kg\,m}^{-1}\,\mathrm{s}^{-1}$

$\mathrm{N_A} = 6.022 \times 10^{23}\,\mathrm{molecules}$

$\omega = 7.27 \times 10^{-5}\,\mathrm{s}^{-1}$

$r_{0,\mathrm{dry}} = 59.49\,\mathrm{nm}$

$R_d = 287.955\,\mathrm{J\,kg}^{-1}\,\mathrm{K}^{-1}$

$R_v = 462.520\,\mathrm{J\,kg}^{-1}\,\mathrm{K}^{-1}$

$R_u = 8.314\,\mathrm{J\,mol}^{-1}\,\mathrm{K}^{-1}$

$\rho_p = 1.5 \times 10^3\,\mathrm{kg\,m}^{-3}$

$\sigma = 5.67 \times 10^{-8}\,\mathrm{W\,m}^{-2}\,\mathrm{K}^{-4}$

$T_0 = 285\,\mathrm{K}$

ACPD

5, 11413–11487, 2005

A3. Parameters

$H_{OH} = 6.9 \times 10^3$ m
$H_{SO2} = 1.2 \times 10^3$ m
$H_{NH3} = 1.2 \times 10^3$ m
$H_{H2SO4} = 1.2 \times 10^3$ m
$H_{N_1} = 1 \times 10^3$ m
$H_{N_2} = 1 \times 10^3$ m
$H_{N_3} = 1 \times 10^3$ m
$H_{M_1} = 1 \times 10^3$ m
$H_{M_2} = 1 \times 10^3$ m
$H_{M_3} = 1 \times 10^3$ m
$H_w = 1.2 \times 10^3$ m
$\overline{[H_2SO_4]}_{min} = 1 \times 10^{11}$ molecules m^{-3}
$\overline{[H_2SO_4]}_{max} = 1 \times 10^{12}$ molecules m^{-3}
$n_{OH} = 6$
$n_w = 2.4$
$\overline{[NH_3]}_{tot,sfc} = 1 \times 10^{-1}$ μg m^{-3}
$\overline{[N_1]}_{sfc} = 1 \times 10^6$ m^{-3}
$\overline{[N_2]}_{sfc} = 10 \times 10^6$ m^{-3}
$\overline{[N_3]}_{sfc} = 10 \times 10^6$ m^{-3}
$\overline{[OH]}_{min} = 2 \times 10^{11}$ molecules m^{-3}
$\overline{[OH]}_{max} = 10 \times 10^{12}$ molecules m^{-3}
$\overline{[SO_2]}_{sfc} = 5$ μg m^{-3}
$u_g = 5$ m s^{-1}
$v_g = 0$ m s^{-1}

ACPD
5, 11413–11487, 2005

$V_{SO_2} = 0.8 \times 10^{-2}\,\mathrm{m\,s^{-1}}$
$V_{NH_3} = 1 \times 10^{-2}\,\mathrm{m\,s^{-1}}$
$V_{H_2SO_4} = 1 \times 10^{-2}\,\mathrm{m\,s^{-1}}$
$\overline{w}_H = -1 \times 10^{-2}\,\mathrm{m\,s^{-1}}$
$z_s = 1\,\mathrm{m}$
$z_p = 10\,\mathrm{m}$

A4. Annotations

$\overline{(\,)}$ – Average over grid cell volume and integration time step
$(\,)'$ – Turbulent deviation from the average
$(\,)_{dry}, (\,)_{wet}$ – Dry and wet particle property, respectively
$(\,)_{tot}$ – Total (gas + aerosol) concentration of species
$(\,)_{sfc}$ – Surface variable
$\widetilde{(\,)}$ – Integration variable
$(\,)_{rad}$ – Radiation – induced
$(\,)_{reac}$ – Chemical reaction – induced
δ_{ij} – Kronecker Delta (Stull, 1997, p. 57)
ε_{ijk} – Alternating unit tensor (Stull, 1997, p. 57)

ACPD
5, 11413–11487, 2005

A5. Abbreviations

CBL – Convective boundary layer
CSL – Convective surface layer
FT – Free troposphere
MBL – Marine boundary layer
NPF – New particle formation
PBL – Planetary boundary layer
PDF – Probability density function
RT – Radiative transfer
SGS – Subgrid scale
UCN – Ultrafine condensation nuclei
UT – Upper troposphere

ACPD
5, 11413–11487, 2005

A6. Scaling properties

$$
\begin{aligned}
u_\star &= \left[\left(\overline{w'u'} \right)_{z_s}^2 + \left(\overline{w'v'} \right)_{z_s}^2 \right]^{1/4} \\
\left(\overline{w'u'} \right)_{z_s} &= - \left[\frac{\overline{u}(z_{k=1})}{\overline{U}(z_{k=1})} \right] u_\star^2 \\
\left(\overline{w'v'} \right)_{z_s} &= - \left[\frac{\overline{v}(z_{k=1})}{\overline{U}(z_{k=1})} \right] u_\star^2 \\
\overline{U}(z_{k=1}) &= \sqrt{\overline{u}(z_{k=1})^2 + \overline{v}(z_{k=1})^2} \\
w_\star &= \begin{cases} \left[\beta_{buo} \left(\overline{w'\theta'} \right)_{z_s} z_i \right]^{1/3}, & \left(\overline{w'\theta'} \right)_{z_s} > 0 \\ 0, & \left(\overline{w'\theta'} \right)_{z_s} < 0 \end{cases} \\
L &= - \frac{u_\star^3}{\kappa \beta_{buo} \left(\overline{w'\theta'} \right)_{z_s}} \\
\theta_\star &= - \left(\overline{w'\theta'} \right)_{z_s} / u_\star \\
q_\star &= - \left(\overline{w'q'} \right)_{z_s} / u_\star \\
\chi_{\alpha\star} &= - \left(\overline{w'\chi'_\alpha} \right)_{z_s} / u_\star \\
\left(\overline{w'\theta'} \right)_{z_s} &= -u_\star \theta_\star \\
\left(\overline{w'q'} \right)_{z_s} &= -u_\star q_\star
\end{aligned}
\tag{A1}
$$

A7. Turbulence-dissipation length scale

(References: André et al., 1978)

$$
\begin{aligned}
\varepsilon &= C_1(L_{\text{turb}})\frac{\overline{e}^{3/2}}{L_{\text{turb}}} \\
C_1(L_{\text{turb}}) &= 0.019 + 0.051\frac{L_{\text{turb}}}{L_{\text{Blackadar}}} \\
L_{\text{turb}} &= \text{Min}(L_{\text{Blackadar}}, L_D) \\
L_{\text{Blackadar}} &= \frac{\kappa z}{1 + \kappa\frac{z}{L_0}} \\
L_0 &= 0.1\frac{\int_0^\infty \sqrt{\overline{e}}z\,dz}{\int_0^\infty \sqrt{\overline{e}}\,dz} \\
L_D &= 0.75\sqrt{\frac{\overline{e}}{\beta_{\text{buo}}\frac{\partial\overline{\theta}}{\partial z}}}
\end{aligned}
\qquad \text{(A2)}
$$

ACPD

5, 11413–11487, 2005

Appendix B

Nonfiltered equations

B1. Meteorological model

$$\frac{du}{dt} = f(v - v_g) \tag{B1}$$

$$\frac{dv}{dt} = -f(u - u_g) \tag{B2}$$

$$\frac{d\theta}{dt} = \left(\frac{\partial\theta}{\partial t}\right)_{\text{rad}} \tag{B3}$$

$$\frac{dq}{dt} = 0 \tag{B4}$$

B2. Chemical model

$$\frac{d\chi_\alpha}{dt} = R_\alpha + Q_\alpha + Q_{\alpha,\text{emission}} \quad , \quad R_\alpha = \sum_{m=1}^{N}\sum_{n=m}^{N} k^\alpha_{mn}\,\chi_m\chi_n \quad , \quad \alpha = 1,\ldots,N \tag{B5}$$

$$\begin{aligned}\frac{d\chi_1}{dt} &= \frac{d[\text{NH}_3]_{\text{tot}}}{dt} \\ &= Q_{1,\text{emission}}\end{aligned} \tag{B6}$$

$$\begin{aligned}\frac{d\chi_2}{dt} &= \frac{d[\text{SO}_2]}{dt} \\ &= \underbrace{-\,k_1\,[\text{OH}]\,[\text{SO}_2]}_{Q_2} + Q_{2,\text{emission}}\end{aligned} \tag{B7}$$

ACPD

5, 11413–11487, 2005

$$\frac{d\chi_3}{dt} = \frac{d[H_2SO_4]}{dt}$$
$$= \underbrace{-\,C_{\mathrm{cond},H_2SO_4}(r_{1,\mathrm{wet}})}_{k_{34}^3}\ \underbrace{[H_2SO_4]}_{\chi_3}\ \underbrace{N_1}_{\chi_4}$$
$$\underbrace{-\,C_{\mathrm{cond},H_2SO_4}(r_{2,\mathrm{wet}})}_{k_{35}^3}\ \underbrace{[H_2SO_4]}_{\chi_3}\ \underbrace{N_2}_{\chi_5}$$
$$\underbrace{-\,C_{\mathrm{cond},H_2SO_4}(r_{3,\mathrm{wet}})}_{k_{36}^3}\ \underbrace{[H_2SO_4]}_{\chi_3}\ \underbrace{N_3}_{\chi_6}$$
$$\underbrace{+\,k_1\,[OH]\,[SO_2]\ -\ J_{\mathrm{nuc}}\,n^*_{H_2SO_4}}_{Q_3} \qquad \text{(B8)}$$

B3. Aerosol model

(References: Pirjola et al., 1999)

$$\frac{d\chi_4}{dt} = \frac{dN_1}{dt}$$
$$= \underbrace{-\frac{1}{2} C_{\mathrm{coag}}(r_{1,\mathrm{wet}}, r_{1,\mathrm{wet}})}_{k^4_{44}} \underbrace{N_1}_{\chi_4} \underbrace{N_1}_{\chi_4}$$
$$\underbrace{- C_{\mathrm{coag}}(r_{1,\mathrm{wet}}, r_{2,\mathrm{wet}})}_{k^4_{45}} \underbrace{N_1}_{\chi_4} \underbrace{N_2}_{\chi_5}$$
$$\underbrace{- C_{\mathrm{coag}}(r_{1,\mathrm{wet}}, r_{3,\mathrm{wet}})}_{k^4_{46}} \underbrace{N_1}_{\chi_4} \underbrace{N_3}_{\chi_6}$$
$$\underbrace{+ J_{\mathrm{nuc}}}_{Q_4} \qquad \text{(B9)}$$

$$\frac{d\chi_5}{dt} = \frac{dN_2}{dt}$$
$$= \underbrace{-\frac{1}{2} C_{\mathrm{coag}}(r_{2,\mathrm{wet}}, r_{2,\mathrm{wet}})}_{k^5_{55}} \underbrace{N_2}_{\chi_5} \underbrace{N_2}_{\chi_5}$$
$$\underbrace{- C_{\mathrm{coag}}(r_{2,\mathrm{wet}}, r_{3,\mathrm{wet}})}_{k^5_{56}} \underbrace{N_2}_{\chi_5} \underbrace{N_3}_{\chi_6} \qquad \text{(B10)}$$

ACPD
5, 11413–11487, 2005

$$\frac{d\chi_6}{dt} = \frac{dN_3}{dt}$$
$$= \underbrace{-\frac{1}{2} C_{\mathrm{coag}}(r_{3,\mathrm{wet}}, r_{3,\mathrm{wet}})}_{k^6_{66}} \underbrace{N_3}_{\chi_6} \underbrace{N_3}_{\chi_6} \tag{B11}$$

$$\frac{d\chi_7}{dt} = \frac{dM_1}{dt}$$
$$= \underbrace{C_{\mathrm{cond},\mathrm{H_2SO_4}}(r_{1,\mathrm{wet}})\, m_{\mathrm{H_2SO_4}}}_{k^7_{34}} \underbrace{[\mathrm{H_2SO_4}]}_{\chi_3} \underbrace{N_1}_{\chi_4}$$
$$\underbrace{- C_{\mathrm{coag}}(r_{1,\mathrm{wet}}, r_{2,\mathrm{wet}})\, m_1}_{k^7_{45}} \underbrace{N_1}_{\chi_4} \underbrace{N_2}_{\chi_5}$$
$$\underbrace{- C_{\mathrm{coag}}(r_{1,\mathrm{wet}}, r_{3,\mathrm{wet}})\, m_1}_{k^7_{46}} \underbrace{N_1}_{\chi_4} \underbrace{N_3}_{\chi_6} \tag{B12}$$
$$\underbrace{+ J_{\mathrm{nuc}}(n^\star_{\mathrm{H_2SO_4}} m_{\mathrm{H_2SO_4}} + n^\star_{\mathrm{NH_3}} m_{\mathrm{NH_3}})}_{Q_7}$$

$$\frac{d\chi_8}{dt} = \frac{dM_2}{dt}$$
$$= \underbrace{C_{\mathrm{cond,H_2SO_4}}(r_{2,\mathrm{wet}})\, m_{\mathrm{H_2SO_4}}}_{k^8_{35}} \underbrace{[\mathrm{H_2SO_4}]}_{\chi_3} \underbrace{N_2}_{\chi_5}$$
$$\underbrace{+\, C_{\mathrm{coag}}(r_{1,\mathrm{wet}}, r_{2,\mathrm{wet}})\, m_1}_{k^8_{45}} \underbrace{N_1}_{\chi_4} \underbrace{N_2}_{\chi_5}$$
$$\underbrace{-\, C_{\mathrm{coag}}(r_{2,\mathrm{wet}}, r_{3,\mathrm{wet}})\, m_2}_{k^8_{56}} \underbrace{N_2}_{\chi_5} \underbrace{N_3}_{\chi_6} \quad \text{(B13)}$$

$$\frac{d\chi_9}{dt} = \frac{dM_3}{dt}$$
$$= \underbrace{C_{\mathrm{cond,H_2SO_4}}(r_{3,\mathrm{wet}})\, m_{\mathrm{H_2SO_4}}}_{k^9_{36}} \underbrace{[\mathrm{H_2SO_4}]}_{\chi_3} \underbrace{N_3}_{\chi_6}$$
$$\underbrace{+\, C_{\mathrm{coag}}(r_{1,\mathrm{wet}}, r_{3,\mathrm{wet}})\, m_1}_{k^9_{46}} \underbrace{N_1}_{\chi_4} \underbrace{N_3}_{\chi_6}$$
$$\underbrace{+\, C_{\mathrm{coag}}(r_{2,\mathrm{wet}}, r_{3,\mathrm{wet}})\, m_2}_{k^9_{56}} \underbrace{N_2}_{\chi_5} \underbrace{N_3}_{\chi_6} \quad \text{(B14)}$$

ACPD
5, 11413–11487, 2005

B4. Condensation coefficient, Fuchs-Sutugin correction for transition regime

(References: Seinfeld and Pandis, 1998, p. 416, 596–597; Clement and Ford, 1999b; Liu et al., 2001)

$$
\begin{aligned}
C_{\mathrm{cond,gas}}(r_{i,\mathrm{wet}}) &= 4\,\pi\,\mathcal{F}_{\mathrm{gas}}(r_{i,\mathrm{wet}})\,D_{\mathrm{gas}}\,r_{i,\mathrm{wet}}\ , \\
&\quad \{\text{“gas”} = \mathrm{H_2SO_4};\ (i = 1, \ldots, 3)\} \\
\mathcal{F}_{\mathrm{gas}}(r_{i,\mathrm{wet}}) &= \frac{f[K\,n_{\mathrm{gas}}(r_{i,\mathrm{wet}})]}{1 + 1.333\,K\,n_{\mathrm{gas}}(r_{i,\mathrm{wet}})\,f[K\,n_{\mathrm{gas}}(r_{i,\mathrm{wet}})]\left(\frac{1}{\alpha_{\mathrm{gas}}} - 1\right)} \\
f[K\,n_{\mathrm{gas}}(r_{i,\mathrm{wet}})] &= \frac{1 + K\,n_{\mathrm{gas}}(r_{i,\mathrm{wet}})}{1 + 1.7\,K\,n_{\mathrm{gas}}(r_{i,\mathrm{wet}}) + 1.333\,[K\,n_{\mathrm{gas}}(r_{i,\mathrm{wet}})]^2} \qquad \text{(B15)} \\
K\,n_{\mathrm{gas}}(r_{i,\mathrm{wet}}) &= \frac{\lambda_{\mathrm{gas}}}{r_{i,\mathrm{wet}}} \\
\lambda_{\mathrm{gas}} &= \frac{3\,D_{\mathrm{gas}}}{\overline{v}_{\mathrm{gas}}} \\
\overline{v}_{\mathrm{gas}} &= \sqrt{\frac{8R_uT}{\pi M_{\mathrm{gas}}}}
\end{aligned}
$$

B5. Brownian coagulation coefficient

(References: Seinfeld and Pandis, 1998, p. 445–456, 474, 661, 662, Fig. 12.5)

$$
\begin{aligned}
C_{\mathrm{coag}}(r_{1,\mathrm{wet}}, r_{2,\mathrm{wet}}) &= 4\pi\,(D_1 + D_2)\,(r_{1,\mathrm{wet}} + r_{2,\mathrm{wet}}) \\
&\quad \times \left\{ \frac{r_{1,\mathrm{wet}} + r_{2,\mathrm{wet}}}{r_{1,\mathrm{wet}} + r_{2,\mathrm{wet}} + (g_1^2 + g_2^2)^{1/2}} \right. \\
&\quad \left. + \frac{4(D_1 + D_2)}{(\overline{v}_1^2 + \overline{v}_2^2)^{1/2}\,(r_{1,\mathrm{wet}} + r_{2,\mathrm{wet}})} \right\}^{-1} \\
D_i &= \frac{kT}{6\pi\mu_{\mathrm{air}} r_{i,\mathrm{wet}}} \left(\frac{5 + 4Kn_i + 6Kn_i^2 + 18Kn_i^3}{5 - Kn_i + (8+\pi)Kn_i^2} \right) \\
Kn_i &= \frac{\lambda_{\mathrm{air}}}{r_{i,\mathrm{wet}}} \\
g_i &= \frac{1}{6\,r_{i,\mathrm{wet}}\,l_i} \left[(2\,r_{i,\mathrm{wet}} + l_i)^3 - (4\,r_{i,\mathrm{wet}}^2 + l_i^2)^{3/2} \right] - 2\,r_{i,\mathrm{wet}} \\
\overline{v}_i &= \sqrt{\frac{8kT}{\pi m_i}} \\
l_i &= \frac{8D_i}{\pi \overline{v}_i}
\end{aligned}
\tag{B16}
$$

ACPD
5, 11413–11487, 2005

B6. Humidity growth

(References: Birmili and Wiedensohler, pers. comm., 2004)

$$
\begin{aligned}
m_i &= \frac{M_i}{N_i}\,, \quad i = 1, \ldots, 3 \\
r_{i,\mathrm{dry}} &= \left(\frac{3m_i}{4\pi\rho_p}\right)^{\frac{1}{3}} \\
r_{i,\mathrm{wet}} &= r_{i,\mathrm{dry}} \times GF(r_{i,\mathrm{dry}}, RH) \\
GF(r_{i,\mathrm{dry}}, RH) &= (1 - RH)^{-\Xi(r_{i,\mathrm{dry}})\,RH} \\
\Xi(r_{i,\mathrm{dry}}) &= \eta_2 + \frac{\eta_1 - \eta_2}{\left(1 + \frac{r_{i,\mathrm{dry}}}{r_{0,\mathrm{dry}}}\right)^{\eta_3}}
\end{aligned}
\tag{B17}
$$

B7. Hydroxyl radical

(References: Liu et al., 2001, see references therein)

$$
\overline{[\mathrm{OH}]} = \overline{[\mathrm{OH}]}_{\min} + \overline{[\mathrm{OH}]}_{\max} \exp\left(-\frac{z}{H_{\mathrm{OH}}}\right)\left[\sin\left(\frac{\pi}{24 \times 3600}t\right)\right]^{n_{\mathrm{OH}}} \tag{B18}
$$

B8. Large-scale subsidence

$$
\overline{w} = \begin{cases} \overline{w}_H \left[1 - \left(1 - \frac{z}{H_w}\right)^{n_w}\right] & , z/H_w \le 1 \\ \overline{w}_H & , z/H_w > 1 \end{cases} \tag{B19}
$$

Appendix C

Filtered equations

(References: André et al., 1976a,b, 1978, 1981)

C1. First moments

$$\frac{\partial \overline{u}}{\partial t} + \overline{w}\frac{\partial \overline{u}}{\partial z} = -\frac{\partial \overline{w'u'}}{\partial z} + f(\overline{v} - v_g) \tag{C1}$$

$$\frac{\partial \overline{v}}{\partial t} + \overline{w}\frac{\partial \overline{v}}{\partial z} = -\frac{\partial \overline{w'v'}}{\partial z} - f(\overline{u} - u_g) \tag{C2}$$

$$\frac{\partial \overline{\theta}}{\partial t} + \overline{w}\frac{\partial \overline{\theta}}{\partial z} = -\frac{\partial \overline{w'\theta'}}{\partial z} + \left(\frac{\partial \overline{\theta}}{\partial t}\right)_{\text{rad}} \tag{C3}$$

$$\frac{\partial \overline{q}}{\partial t} + \overline{w}\frac{\partial \overline{q}}{\partial z} = -\frac{\partial \overline{w'q'}}{\partial z} \tag{C4}$$

$$\frac{\partial \overline{\chi}_\alpha}{\partial t} + \overline{w}\frac{\partial \overline{\chi}_\alpha}{\partial z} = -\frac{\partial \overline{w'\chi'_\alpha}}{\partial z} + \overline{R}_\alpha + \overline{Q}_\alpha \,, \tag{C5}$$

$$\overline{R}_\alpha = \sum_{m=1}^{N}\sum_{n=m}^{N} \overline{k}^{\alpha}_{mn}\left(\overline{\chi}_m\overline{\chi}_n + \overline{\chi'_m\chi'_n}\right) \,, \quad \alpha = 1, \ldots, N$$

ACPD
5, 11413–11487, 2005

C2. Second-order moment equations

C2.1. The six velocity correlations $\{\ \overline{u'u'},\ \overline{u'v'},\ \overline{u'w'},\ \overline{v'v'},\ \overline{v'w'},\ \overline{w'w'}\ \}$

$$\frac{\partial \overline{u_i' u_j'}}{\partial t} + \overline{w}\frac{\partial \overline{u_i' u_j'}}{\partial z} = -\frac{\partial \overline{u_i' u_j' w'}}{\partial z} - \left(\overline{u_i' w'}\frac{\partial \overline{u}_j}{\partial z} + \overline{u_j' w'}\frac{\partial \overline{u}_i}{\partial z}\right)$$
$$+\beta_{\text{buo}}\left(\delta_{3j}\overline{u_i'\theta_v'} + \delta_{3i}\overline{u_j'\theta_v'}\right) + f\left(\epsilon_{ik3}\overline{u_j' u_k'} + \epsilon_{jk3}\overline{u_i' u_k'}\right) \qquad \text{(C6)}$$
$$-\frac{1}{\rho_0}\left(\overline{u_i'\frac{\partial p'}{\partial x_j} + u_j'\frac{\partial p'}{\partial x_i}}\right) - \frac{2}{3}\delta_{ij}\varepsilon$$

$$-\frac{1}{\rho_0}\left(\overline{u_i'\frac{\partial p'}{\partial x_j} + u_j'\frac{\partial p'}{\partial x_i}}\right) = -C_4\frac{\varepsilon}{\overline{e}}\left(\overline{u_i' u_j'} - \frac{2}{3}\delta_{ij}\overline{e}\right) - C_5\left(P_{ij} - \frac{2}{3}\delta_{ij}P\right)$$

$$P_{ij} = \beta_{\text{buo}}\left(\delta_{3j}\overline{u_i'\theta_v'} + \delta_{3i}\overline{u_j'\theta_v'}\right) - \left(\overline{u_i' w'}\frac{\partial \overline{u}_j}{\partial z} + \overline{u_j' w'}\frac{\partial \overline{u}_i}{\partial z}\right) \qquad \text{(C7)}$$

$$P = \beta_{\text{buo}}\overline{w'\theta_v'} - \overline{u'w'}\frac{\partial \overline{u}}{\partial z} - \overline{v'w'}\frac{\partial \overline{v}}{\partial z}$$

$$\overline{e} = \frac{1}{2}\overline{u_k' u_k'}$$
$$\varepsilon = C_1(L_{\text{turb}})\frac{\overline{e}^{3/2}}{L_{\text{turb}}} \qquad \text{(C8)}$$

ACPD
5, 11413–11487, 2005

C2.2. Scalar fluxes $\{\ \overline{u_i' a'},\ \ u_i=(u,v,w),\ \ a=(\theta, q, \chi_\alpha, \alpha=1,\ldots,N\ \}$

$$\frac{\partial \overline{u_i' a'}}{\partial t} + \overline{w}\frac{\partial \overline{u_i' a'}}{\partial z} = -\frac{\partial \overline{u_i' w' a'}}{\partial z} - \left(\overline{u_i' w'}\frac{\partial \overline{a}}{\partial z} + \overline{w' a'}\frac{\partial \overline{u}_i}{\partial z}\right) + \delta_{3i}\beta_{\mathrm{buo}}\overline{\theta_v' a'} + \epsilon_{ik3} f \overline{u_k' a'} - \frac{1}{\rho_0}\overline{a'\frac{\partial p'}{\partial x_i}} + \left.\frac{\partial \overline{u_i' a'}}{\partial t}\right|_{\mathrm{reac}} \tag{C9}$$

$$-\frac{1}{\rho_0}\overline{a'\frac{\partial p'}{\partial x_i}} = -C_6\frac{\varepsilon}{\overline{e}}\overline{u_i' a'} - C_7 P_{ia}$$

$$P_{ia} = \delta_{3i}\beta_{\mathrm{buo}}\overline{\theta_v' a'} - \overline{w' a'}\frac{\partial \overline{u}_i}{\partial z} \tag{C10}$$

The reaction term in the tracer flux equation $\{a=\chi_\alpha\}$ follows from Eq. (C20), i.e.,

$$\left.\frac{\partial \overline{u_i' \chi_\alpha'}}{\partial t}\right|_{\mathrm{reac}} = \overline{R}_{u_i \chi_\alpha} = \sum_{m=1}^{N}\sum_{n=m}^{N} \overline{k}_{mn}^{\alpha}\left(\overline{\chi}_m \overline{u_i' \chi_n'} + \overline{\chi}_n \overline{u_i' \chi_m'} + \overline{u_i' \chi_m' \chi_n'}\right)\ . \tag{C11}$$

C2.3. Scalar correlations $\{\ \overline{a' b'},\ \ (a,b)=(\theta, q, \chi_\alpha, \chi_\beta, (\alpha,\beta)=1,\ldots,N)\ \}$

$$\frac{\partial \overline{a' b'}}{\partial t} + \overline{w}\frac{\partial \overline{a' b'}}{\partial z} = -\frac{\partial \overline{w' a' b'}}{\partial z} - \left\{\overline{w' a'}\frac{\partial \overline{b}}{\partial z} + \overline{w' b'}\frac{\partial \overline{a}}{\partial z}\right\} - \varepsilon_{ab} - \varepsilon_R + \left.\frac{\partial \overline{a' b'}}{\partial t}\right|_{\mathrm{reac}} \tag{C12}$$

$$\varepsilon_{ab} = C_2\frac{\varepsilon}{\overline{e}}\overline{a' b'} \tag{C13}$$

ACPD
5, 11413–11487, 2005

The radiative destruction rate ε_R appears only in the temperature variance equation, i.e.,

$$\varepsilon_R = c_R \overline{\theta'\theta'} \ , \quad c_R \approx \left(0.036 \frac{\mathrm{m}}{\mathrm{s}}\right) \frac{\varepsilon}{\overline{e}^{3/2}} \ , \quad c_R = \left[\frac{1}{\mathrm{s}}\right] \tag{C14}$$

(Stull, 1997, p. 132, see references therein). The interaction term between passive and reactive scalar $\{a{=}(\theta, q),\ b{=}\chi_\alpha\}$ follows from Eq. (C20), i.e.,

$$\left.\frac{\partial \overline{a'\chi'_\alpha}}{\partial t}\right|_{\mathrm{reac}} = \overline{R}_{a\chi_\alpha} = \sum_{m=1}^{N}\sum_{n=m}^{N} \overline{k}^{\alpha}_{mn} \left(\overline{\chi}_m \overline{a'\chi'_n} + \overline{\chi}_n \overline{a'\chi'_m} + \overline{a'\chi'_m\chi'_n}\right) \ . \tag{C15}$$

The interaction between two reactive scalars $\{(a,\ b){=}(\chi_\alpha,\ \chi_\beta\}$, results from Eq. (C25), i.e.,

$$\left.\frac{\partial \overline{\chi'_\alpha\chi'_\beta}}{\partial t}\right|_{\mathrm{reac}} = \overline{R}_{\chi_\alpha\chi_\beta} \ . \tag{C16}$$

C2.4. Interaction of a reactive tracer χ_α with a nonreactive scalar $A{=}(u_i, \theta, q)$

$$\begin{aligned} \left.\frac{\partial \chi_\alpha}{\partial t}\right|_{\mathrm{reac}} &= \sum_{m=1}^{N}\sum_{n=m}^{N} k^{\alpha}_{mn}\chi_m\chi_n && | \times A \\ + \left.\frac{\partial A}{\partial t}\right|_{\mathrm{reac}} &= 0 && | \times \chi_\alpha \\ \hline \left.\frac{\partial A\chi_\alpha}{\partial t}\right|_{\mathrm{reac}} &= \sum_{m=1}^{N}\sum_{n=m}^{N} k^{\alpha}_{mn} A\chi_m\chi_n && | \ \overline{(\ \ )}\ ; \quad \text{averaging} \ . \end{aligned} \tag{C17}$$

$$\left.\frac{\partial}{\partial t}\left(\overline{A}\overline{\chi}_\alpha + \overline{A'\chi'_\alpha}\right)\right|_{\text{reac}} = \sum_{m=1}^{N}\sum_{n=m}^{N} \overline{k}^{\alpha}_{mn}\overline{A}\left(\overline{\chi}_m\overline{\chi}_n + \overline{\chi'_m\chi'_n}\right)$$
$$+ \sum_{m=1}^{N}\sum_{n=m}^{N} \overline{k}^{\alpha}_{mn}\left(\overline{\chi}_m\overline{A'\chi'_n} + \overline{\chi}_n\overline{A'\chi'_m} + \overline{A'\chi'_m\chi'_n}\right) . \quad \text{(C18)}$$

$$\left.\frac{\partial\overline{\chi}_\alpha}{\partial t}\right|_{\text{reac}} = \sum_{m=1}^{N}\sum_{n=m}^{N} \overline{k}^{\alpha}_{mn}\left(\overline{\chi}_m\overline{\chi}_n + \overline{\chi'_m\chi'_n}\right) \quad | \times \overline{A}$$
$$+ \frac{\partial\overline{A}}{\partial t} = 0 \quad | \times \overline{\chi}_\alpha \quad \text{(C19)}$$

$$\left.\frac{\partial\overline{A}\overline{\chi}_\alpha}{\partial t}\right|_{\text{reac}} = \sum_{m=1}^{N}\sum_{n=m}^{N} \overline{k}^{\alpha}_{mn}\overline{A}\left(\overline{\chi}_m\overline{\chi}_n + \overline{\chi'_m\chi'_n}\right) \quad | \overline{(\ )}\,; \quad \text{averaging}$$

Subtracting Eq. (C19) from Eq. (C18):

$$\overline{R}_{A\chi_\alpha} = \left.\frac{\partial\overline{A'\chi'_\alpha}}{\partial t}\right|_{\text{reac}} = \sum_{m=1}^{N}\sum_{n=m}^{N} \overline{k}^{\alpha}_{mn}\left(\overline{\chi}_m\overline{A'\chi'_n} + \overline{\chi}_n\overline{A'\chi'_m} + \overline{A'\chi'_m\chi'_n}\right) \quad \text{(C20)}$$

C2.5. Interaction of reactive tracers χ_α and χ_β

$$\left.\frac{\partial \chi_\alpha}{\partial t}\right|_{\text{reac}} = \sum_{m=1}^{N}\sum_{n=m}^{N} k^{\alpha}_{mn}\chi_m\chi_n \qquad |\times \chi_\beta$$

$$+\left.\frac{\partial \chi_\beta}{\partial t}\right|_{\text{reac}} = \sum_{m=1}^{N}\sum_{n=m}^{N} k^{\beta}_{mn}\chi_m\chi_n \qquad |\times \chi_\alpha$$

$$\left.\frac{\partial \chi_\alpha\chi_\beta}{\partial t}\right|_{\text{reac}} = \sum_{m=1}^{N}\sum_{n=m}^{N} k^{\alpha}_{mn}\chi_\beta\chi_m\chi_n + \sum_{m=1}^{N}\sum_{n=m}^{N} k^{\beta}_{mn}\chi_\alpha\chi_m\chi_n \qquad |\overline{(\ )} \tag{C21}$$

$$\left.\frac{\partial \overline{\chi_\alpha\chi_\beta}}{\partial t}\right|_{\text{reac}} = \sum_{m=1}^{N}\sum_{n=m}^{N} \overline{k}^{\alpha}_{mn}\,\overline{\chi_\beta\chi_m\chi_n} + \sum_{m=1}^{N}\sum_{n=m}^{N} \overline{k}^{\beta}_{mn}\,\overline{\chi_\alpha\chi_m\chi_n}\,.$$

Expanding the last equation using:

$$\begin{aligned}
\overline{ABC} &= \overline{(\overline{A}+A')(\overline{B}+B')(\overline{C}+C')} \\
&= \overline{A}\,\overline{B}\,\overline{C} + \overline{A}\,\overline{B'C'} + \overline{B}\,\overline{A'C'} + \overline{C}\,\overline{A'B'} + \overline{A'B'C'}\,, \\
\overline{\chi_\alpha\chi_m\chi_n} &= \overline{\chi}_\alpha\overline{\chi}_m\overline{\chi}_n + \overline{\chi}_\alpha\overline{\chi'_m\chi'_n} + \overline{\chi}_m\overline{\chi'_\alpha\chi'_n} + \overline{\chi}_n\overline{\chi'_\alpha\chi'_m} + \overline{\chi'_\alpha\chi'_m\chi'_n}\,, \\
\overline{\chi_\beta\chi_m\chi_n} &= \overline{\chi}_\beta\overline{\chi}_m\overline{\chi}_n + \overline{\chi}_\beta\overline{\chi'_m\chi'_n} + \overline{\chi}_m\overline{\chi'_\beta\chi'_n} + \overline{\chi}_n\overline{\chi'_\beta\chi'_m} + \overline{\chi'_\beta\chi'_m\chi'_n}
\end{aligned} \tag{C22}$$

$$\left.\frac{\partial}{\partial t}\left(\overline{\chi}_\alpha\overline{\chi}_\beta+\overline{\chi'_\alpha\chi'_\beta}\right)\right|_{\text{reac}}=$$

$$\sum_{m=1}^{N}\sum_{n=m}^{N}\overline{k}^{\alpha}_{mn}\left(\overline{\chi}_\beta\overline{\chi}_m\overline{\chi}_n+\overline{\chi}_\beta\overline{\chi'_m\chi'_n}+\overline{\chi}_m\overline{\chi'_\beta\chi'_n}+\overline{\chi}_n\overline{\chi'_\beta\chi'_m}+\overline{\chi'_\beta\chi'_m\chi'_n}\right)$$

$$+\sum_{m=1}^{N}\sum_{n=m}^{N}\overline{k}^{\beta}_{mn}\left(\overline{\chi}_\alpha\overline{\chi}_m\overline{\chi}_n+\overline{\chi}_\alpha\overline{\chi'_m\chi'_n}+\overline{\chi}_m\overline{\chi'_\alpha\chi'_n}+\overline{\chi}_n\overline{\chi'_\alpha\chi'_m}+\overline{\chi'_\alpha\chi'_m\chi'_n}\right) \tag{C23}$$

Contribution of the mean values to the total change rate:

$$\left.\frac{\partial\overline{\chi}_\alpha}{\partial t}\right|_{\text{reac}}=\sum_{m=1}^{N}\sum_{n=m}^{N}\overline{k}^{\alpha}_{mn}\left(\overline{\chi}_m\overline{\chi}_n+\overline{\chi'_m\chi'_n}\right)\qquad|\times\overline{\chi}_\beta$$

$$+\left.\frac{\partial\overline{\chi}_\beta}{\partial t}\right|_{\text{reac}}=\sum_{m=1}^{N}\sum_{n=m}^{N}\overline{k}^{\beta}_{mn}\left(\overline{\chi}_m\overline{\chi}_n+\overline{\chi'_m\chi'_n}\right)\qquad|\times\overline{\chi}_\alpha$$

$$\left.\frac{\partial\overline{\chi}_\alpha\overline{\chi}_\beta}{\partial t}\right|_{\text{reac}}=\sum_{m=1}^{N}\sum_{n=m}^{N}\overline{k}^{\alpha}_{mn}\overline{\chi}_\beta\left(\overline{\chi}_m\overline{\chi}_n+\overline{\chi'_m\chi'_n}\right)+\sum_{m=1}^{N}\sum_{n=m}^{N}\overline{k}^{\beta}_{mn}\overline{\chi}_\alpha\left(\overline{\chi}_m\overline{\chi}_n+\overline{\chi'_m\chi'_n}\right) \tag{C24}$$

Substraction of Eq. (C24) from Eq. (C23) to extract the contribution of the tracer covariance to the total change rate:

$$\overline{R}_{\chi_\alpha\chi_\beta} = \left.\frac{\partial\overline{\chi'_\alpha\chi'_\beta}}{\partial t}\right|_{\text{reac}} = \sum_{m=1}^{N}\sum_{n=m}^{N}\overline{k}^{\alpha}_{mn}\left(\overline{\chi}_m\overline{\chi'_\beta\chi'_n} + \overline{\chi}_n\overline{\chi'_\beta\chi'_m} + \overline{\chi'_\beta\chi'_m\chi'_n}\right) + \sum_{m=1}^{N}\sum_{n=m}^{N}\overline{k}^{\beta}_{mn}\left(\overline{\chi}_m\overline{\chi'_\alpha\chi'_n} + \overline{\chi}_n\overline{\chi'_\alpha\chi'_m} + \overline{\chi'_\alpha\chi'_m\chi'_n}\right) \tag{C25}$$

C3. Third-order moment equations

C3.1. Turbulent transport of momentum fluxes $\{\ \overline{u'u'w'}, \overline{u'v'w'}, \overline{u'w'w'}, \overline{v'v'w'}, \overline{v'w'w'}, \overline{w'w'w'}\ \}$

$$\frac{\partial\overline{u'_iu'_jw'}}{\partial t} + \overline{w}\frac{\partial\overline{u'_iu'_jw'}}{\partial z} = -\left(\overline{u'_iw'w'}\frac{\partial\overline{u}_j}{\partial z} + \overline{u'_jw'w'}\frac{\partial\overline{u}_i}{\partial z}\right) - \overline{w'w'}\frac{\partial\overline{u'_iu'_j}}{\partial z} - \left(\overline{u'_iw'}\frac{\partial\overline{u'_jw'}}{\partial z} + \overline{u'_jw'}\frac{\partial\overline{u'_iw'}}{\partial z}\right) + \beta_{\text{buo}}\left(\overline{u'_iu'_j\theta'_v} + \delta_{3j}\overline{u'_iw'\theta'_v} + \delta_{3i}\overline{u'_jw'\theta'_v}\right) - \frac{1}{\rho_0}\left(\overline{u'_iu'_j}\frac{\partial p'}{\partial z} + \overline{u'_iw'}\frac{\partial p'}{\partial x_j} + \overline{u'_jw'}\frac{\partial p'}{\partial x_i}\right) - \varepsilon_{uuu} \tag{C26}$$

ACPD
5, 11413–11487, 2005

$$-\frac{1}{\rho_0}\left(\overline{u_i' u_j' \frac{\partial p'}{\partial z}} + \overline{u_i' w' \frac{\partial p'}{\partial x_j}} + \overline{u_j' w' \frac{\partial p'}{\partial x_i}}\right) = \underbrace{P_{\text{relax}}}_{\text{Andre et al., 1978}} + \underbrace{P_{\text{rapid}}}_{\text{Andre et al., 1981}}$$

$$P_{\text{relax}} = -C_8 \frac{\varepsilon}{e} \overline{u_i' u_j' w'} \tag{C27}$$

$$P_{\text{rapid}} = -C_{11} \beta_{\text{buo}} \left(\overline{u_i' u_j' \theta_v'} + \delta_{3j} \overline{u_i' w' \theta_v'} + \delta_{3i} \overline{u_j' w' \theta_v'}\right)$$

$$\varepsilon_{uuu} = 0$$

$$\left|\overline{u_i' u_j' w'}\right| \leq \text{Min} \left\{ \begin{array}{l} \sqrt{\overline{u_i'^2}\left(\overline{u_j'^2}\,\overline{w'^2} + \overline{u_j' w'}^2\right)} \\ \sqrt{\overline{u_j'^2}\left(\overline{u_i'^2}\,\overline{w'^2} + \overline{u_i' w'}^2\right)} \\ \sqrt{\overline{w'^2}\left(\overline{u_i'^2}\,\overline{u_j'^2} + \overline{u_i' u_j'}^2\right)} \end{array} \right\} . \tag{C28}$$

ACPD
5, 11413–11487, 2005

C3.2. Turbulent transport of scalar fluxes ("fluxes of fluxes")

$\{\ \overline{u_i' u_j' a'},\ \ a=(\theta, q, \chi_\alpha, \alpha=1,\ldots,N)\ \}$

$$\frac{\partial \overline{u_i' u_j' a'}}{\partial t} + \overline{w}\frac{\partial \overline{u_i' u_j' a'}}{\partial z} = -\left(\overline{u_i' u_j' w'}\frac{\partial \overline{a}}{\partial z} + \overline{u_i' w' a'}\frac{\partial \overline{u}_j}{\partial z} + \overline{u_j' w' a'}\frac{\partial \overline{u}_i}{\partial z}\right)$$
$$-\left(\overline{w' a'}\frac{\partial \overline{u_i' u_j'}}{\partial z} + \overline{u_i' w'}\frac{\partial \overline{u_j' a'}}{\partial z} + \overline{u_j' w'}\frac{\partial \overline{u_i' a'}}{\partial z}\right)$$
$$+\beta_{\mathrm{buo}}\left(\delta_{3j}\overline{u_i' \theta_v' a'} + \delta_{3i}\overline{u_j' \theta_v' a'}\right)$$
$$-\frac{1}{\rho_0}\left(\overline{u_i' a'}\frac{\partial p'}{\partial x_j} + \overline{u_j' a'}\frac{\partial p'}{\partial x_i}\right) - \varepsilon_{\mathrm{uua}} \qquad \text{(C29)}$$

$$-\frac{1}{\rho_0}\left(\overline{u_i' a'}\frac{\partial p'}{\partial x_j} + \overline{u_j' a'}\frac{\partial p'}{\partial x_i}\right) = \underbrace{P_{\mathrm{relax}} + P_{\mathrm{diagonal}}}_{\text{Andre et al., 1978}} + \underbrace{P_{\mathrm{rapid}}}_{\text{Andre et al., 1981}}$$

$$P_{\mathrm{relax}} = -C_8\frac{\varepsilon}{e}\left(\overline{u_i' u_j' a'} - \frac{1}{3}\delta_{ij}\overline{u_k' u_k' a'}\right)$$

$$P_{\mathrm{diagonal}} = \delta_{ij} C_9 \frac{\varepsilon}{e}\overline{u_k' u_k' a'} \qquad \text{(C30)}$$

$$P_{\mathrm{rapid}} = -C_{11}\beta_{\mathrm{buo}}\left(\delta_{3j}\overline{u_i' \theta_v' a'} + \delta_{3i}\overline{u_j' \theta_v' a'} - \frac{2}{3}\delta_{ij}\overline{w' \theta_v' a'}\right)$$

$$\varepsilon_{\mathrm{uua}} = \delta_{ij} C_{10}\frac{\varepsilon}{e}\frac{\overline{u_k' u_k' a'}}{3}$$

ACPD
5, 11413–11487, 2005

$$\left|\overline{u_i' u_j' a'}\right| \le \mathrm{Min}\left\{\begin{array}{l}\sqrt{\overline{u_i'^2}\left(\overline{u_j'^2}\,\overline{a'^2}+\overline{u_j' a'}^2\right)}\\ \sqrt{\overline{u_j'^2}\left(\overline{u_i'^2}\,\overline{a'^2}+\overline{u_i' a'}^2\right)}\\ \sqrt{\overline{a'^2}\left(\overline{u_i'^2}\,\overline{u_j'^2}+\overline{u_i' u_j'}^2\right)}\end{array}\right\}. \tag{C31}$$

C3.3. Turbulent transport of scalar correlations ("fluxes of correlations")

$\{\ \overline{u_i' a' b'},\ \ (a,b)=(\theta, q, \chi_\alpha, \chi_\beta, [\alpha,\beta]=1,\ldots,N)\ \}$

$$\begin{aligned}\frac{\partial \overline{u_i' a' b'}}{\partial t}+\overline{w}\frac{\partial \overline{u_i' a' b'}}{\partial z} &= -\left(\overline{w' a' b'}\frac{\partial \overline{u}_i}{\partial z}+\overline{u_i' w' a'}\frac{\partial \overline{b}}{\partial z}+\overline{u_i' w' b'}\frac{\partial \overline{a}}{\partial z}\right)\\ &\quad -\left(\overline{u_i' w'}\frac{\partial \overline{a' b'}}{\partial z}+\overline{w' a'}\frac{\partial \overline{u_i' b'}}{\partial z}+\overline{w' b'}\frac{\partial \overline{u_i' a'}}{\partial z}\right)\\ &\quad +\delta_{3i}\beta_{\mathrm{buo}}\overline{\theta_v' a' b'}-\frac{1}{\rho_0}\left(\overline{a' b'\frac{\partial p'}{\partial x_i}}\right)-\varepsilon_{\mathrm{uab}}\end{aligned} \tag{C32}$$

$$-\frac{1}{\rho_0}\left(\overline{a' b'\frac{\partial p'}{\partial x_i}}\right)=\underbrace{P_{\mathrm{relax}}}_{\text{Andre et al., 1978}}+\underbrace{P_{\mathrm{rapid}}}_{\text{Andre et al., 1981}}$$

$$\begin{aligned}P_{\mathrm{relax}} &= -C_8\frac{\varepsilon}{e}\overline{u_i' a' b'}\\ P_{\mathrm{rapid}} &= -\delta_{3i}C_{11}\beta_{\mathrm{buo}}\overline{a' b'\theta_v'}\\ \varepsilon_{\mathrm{uab}} &= 0\end{aligned} \tag{C33}$$

$$\left|\overline{u_i' a' b'}\right| \le \mathrm{Min}\left\{\begin{array}{l} \sqrt{\overline{u_i'^2}\left(\overline{a'^2}\,\overline{b'^2}+\overline{a'b'}^2\right)} \\ \sqrt{\overline{a'^2}\left(\overline{u_i'^2}\,\overline{b'^2}+\overline{u_i'b'}^2\right)} \\ \sqrt{\overline{b'^2}\left(\overline{u_i'^2}\,\overline{a'^2}+\overline{u_i'a'}^2\right)} \end{array}\right\} \tag{C34}$$

C3.4. Turbulent transport of scalar correlations

$\{\ \overline{a'b'c'},\ (a,b,c)=(\theta,q,\chi_\alpha,\chi_\beta,\chi_\gamma,[\alpha,\beta,\gamma]=1,\ldots,N\ \}$

$$\frac{\partial \overline{a'b'c'}}{\partial t}+\overline{w}\frac{\partial \overline{a'b'c'}}{\partial z} = -\left(\overline{w'a'b'}\frac{\partial \overline{c}}{\partial z}+\overline{w'a'c'}\frac{\partial \overline{b}}{\partial z}+\overline{w'b'c'}\frac{\partial \overline{a}}{\partial z}\right) - \left(\overline{w'a'}\frac{\partial \overline{b'c'}}{\partial z}+\overline{w'b'}\frac{\partial \overline{a'c'}}{\partial z}+\overline{w'c'}\frac{\partial \overline{a'b'}}{\partial z}\right)-\varepsilon_{\mathrm{abc}} \tag{C35}$$

$$\varepsilon_{\mathrm{abc}} = C_{10}\frac{\varepsilon}{\overline{e}}\overline{a'b'c'} \tag{C36}$$

$$\left|\overline{a'b'c'}\right| \le \mathrm{Min}\left\{\begin{array}{l} \sqrt{\overline{a'^2}\left(\overline{b'^2}\,\overline{c'^2}+\overline{b'c'}^2\right)} \\ \sqrt{\overline{b'^2}\left(\overline{a'^2}\,\overline{c'^2}+\overline{a'c'}^2\right)} \\ \sqrt{\overline{c'^2}\left(\overline{a'^2}\,\overline{b'^2}+\overline{a'b'}^2\right)} \end{array}\right\} \tag{C37}$$

C4. Buoyancy fluxes

$$\begin{aligned} \theta_v &= \theta\,(1 + 0.61q) \\ &= \theta + C_{T_0}\,q \\ C_{T_0} &\approx 0.61\,T_0 \\ \overline{a'\theta'_v} &= \overline{a'\theta'} + C_{T_0}\,\overline{a'q'} \\ \overline{a'b'\theta'_v} &= \overline{a'b'\theta'} + C_{T_0}\,\overline{a'b'q'} \end{aligned} \tag{C38}$$

Appendix D

Initial and boundary conditions

D1. First moments

D1.1. Initial conditions

(References: Liu et al., 2001, for chemical variables)

Initial profiles of meteorological variables, i.e.,

$$\overline{u}(z, t_0)\,, \quad \overline{v}(z, t_0)\,, \quad \overline{\theta}(z, t_0)\,, \quad \overline{q}(z, t_0) \tag{D1}$$

can be either derived from observations or prescribed. The geostrophic wind components u_g, v_g, and the large-scale subsidence velocity w_0 are prescribed. The first-order

moments of physico-chemical variables are initialized as follows:

$$
\begin{aligned}
\overline{[\mathrm{OH}]}(z,t_0) &= \overline{[\mathrm{OH}]}_{\min} + \overline{[\mathrm{OH}]}_{\max} \exp\left(-\frac{z}{H_{\mathrm{OH}}}\right)\left[\sin\left(\frac{\pi}{24\times 3600}t_0\right)\right]^{n_{\mathrm{OH}}} \\
\overline{[\mathrm{SO_2}]}(z,t_0) &= \overline{[\mathrm{SO_2}]}_{\mathrm{sfc}} \exp\left(-\frac{z}{H_{\mathrm{SO_2}}}\right) \\
\overline{[\mathrm{NH_3}]}_{\mathrm{tot}}(z,t_0) &= \overline{[\mathrm{NH_3}]}_{\mathrm{tot,sfc}} \exp\left(-\frac{z}{H_{\mathrm{NH_3}}}\right) \\
\overline{[\mathrm{H_2SO_4}]}(z,t_0) &= \overline{[\mathrm{H_2SO_4}]}_{\min} + \overline{[\mathrm{H_2SO_4}]}_{\max} \exp\left(-\frac{z}{H_{\mathrm{H_2SO_4}}}\right)\sin\left(\frac{\pi}{24\times 3600}t_0\right) \\
\overline{N}_i(z,t_0) &= \overline{N}_{i,\mathrm{sfc}} \exp\left(-\frac{z}{H_{N_i}}\right), \quad i = 1,3 \\
\overline{M}_i(z,t_0) &= \overline{M}_{i,\mathrm{sfc}} \exp\left(-\frac{z}{H_{M_i}}\right), \quad i = 1,3
\end{aligned}
\tag{D2}
$$

D1.2. Lower boundary conditions ("constant flux layer" hypothesis)

$$
\begin{aligned}
\left(\overline{u'w'}\right)_{z_s} &\approx \left(\overline{u'w'}\right)_{z_p} \approx -K_m \left.\frac{\partial \overline{u}}{\partial z}\right|_{z_p} \\
\left(\overline{v'w'}\right)_{z_s} &\approx \left(\overline{v'w'}\right)_{z_p} \approx -K_m \left.\frac{\partial \overline{v}}{\partial z}\right|_{z_p} \\
\left(\overline{w'\theta'}\right)_{z_s} &\approx \left(\overline{w'\theta'}\right)_{z_p} \approx -K_h \left.\frac{\partial \overline{\theta}}{\partial z}\right|_{z_p} \\
\left(\overline{w'q'}\right)_{z_s} &\approx \left(\overline{w'q'}\right)_{z_p} \approx -K_h \left.\frac{\partial \overline{q}}{\partial z}\right|_{z_p} \\
\left(\overline{w'\chi'_\alpha}\right)_{z_s} &\approx \left(\overline{w'\chi'_\alpha}\right)_{z_p} \approx -K_h \left.\frac{\partial \overline{\chi_\alpha}}{\partial z}\right|_{z_p}, \quad (\alpha = 1, \ldots, N)
\end{aligned}
\tag{D3}
$$

$$
\begin{aligned}
K_m &= \frac{c_m u_\star z}{\phi_m(\zeta)} \\
K_h &= \frac{c_h u_\star z}{\phi_h(\zeta)}
\end{aligned}
\tag{D4}
$$

ACPD
5, 11413–11487, 2005

$$\left.\frac{\partial \overline{u}}{\partial z}\right|_{z_p} = \left[\frac{\overline{u}(z_{k=1})}{\overline{U}(z_{k=1})}\right] \frac{u_\star}{c_m z_p} \phi_m(\zeta)$$

$$\left.\frac{\partial \overline{v}}{\partial z}\right|_{z_p} = \left[\frac{\overline{v}(z_{k=1})}{\overline{U}(z_{k=1})}\right] \frac{u_\star}{c_m z_p} \phi_m(\zeta)$$

$$\left.\frac{\partial \overline{\theta}}{\partial z}\right|_{z_p} = \frac{\theta_\star}{c_h z_p} \phi_h(\zeta) \qquad \text{(D5)}$$

$$\left.\frac{\partial \overline{q}}{\partial z}\right|_{z_p} = \frac{q_\star}{c_h z_p} \phi_h(\zeta)$$

$$\left.\frac{\partial \overline{\chi}_\alpha}{\partial z}\right|_{z_p} = \frac{\chi_{\alpha\star}}{c_h z_p} \phi_h(\zeta)\,, \quad (\alpha = 1, \ldots, N)$$

D1.3. Similarity functions

(References: Dyer and Hicks, 1970)

$$\phi_m = \begin{cases} (1 - 16\zeta)^{-1/4}\,, & \zeta < 0 \\ (1 + 5\zeta)\,, & \zeta \geq 0 \end{cases} \qquad \text{(D6)}$$

$$\phi_h = \begin{cases} (1 - 16\zeta)^{-1/2}\,, & \zeta < 0 \\ (1 + 5\zeta)\,, & \zeta \geq 0 \end{cases}$$

ACPD
5, 11413–11487, 2005

D1.4. Skin properties

(References: Holtslag, 1987, p. 55–56, 70)

$$\theta_\star = -\frac{\left(\overline{w'\theta'}\right)_{z_s}}{u_\star} = \kappa\Delta\overline{\theta}\left[\ln\left(\frac{z_p}{z_s}\right) - \Psi_H\left(\frac{z_p}{L}\right) + \Psi_H\left(\frac{z_s}{L}\right)\right]^{-1}$$

$$q_\star = -\frac{\left(\overline{w'q'}\right)_{z_s}}{u_\star} = \kappa\Delta\overline{q}\left[\ln\left(\frac{z_p}{z_s}\right) - \Psi_H\left(\frac{z_p}{L}\right) + \Psi_H\left(\frac{z_s}{L}\right)\right]^{-1} \quad \text{(D7)}$$

$$\Delta\overline{\theta} = \overline{\theta}(z_p) - \overline{\theta}(z_s)$$

$$\Delta\overline{q} = \overline{q}(z_p) - \overline{q}(z_s)$$

$$\overline{\theta}(z_s) = \overline{\theta}(z_p) - \frac{\theta_\star}{\kappa}\left[\ln\left(\frac{z_p}{z_s}\right) - \Psi_H\left(\frac{z_p}{L}\right) + \Psi_H\left(\frac{z_s}{L}\right)\right]$$

$$\overline{q}(z_s) = \overline{q}(z_p) - \frac{q_\star}{\theta_\star}\left(\overline{\theta}(z_p) - \overline{\theta}(z_s)\right) \quad \text{(D8)}$$

$$\frac{\Delta\overline{\theta}}{\overline{\theta}} = \frac{\Delta\overline{T}}{\overline{T}} + \frac{g}{c_p}\frac{\Delta z}{\overline{T}} \quad \text{(D9)}$$

$$\Delta\overline{T} \approx \Delta\overline{\theta} - \Gamma_d(z_p - z_s)$$

ACPD

5, 11413–11487, 2005

D1.5. Stability function

(References: Paulson, 1970, unstable case; Carson and Richards, 1978, stable case; Holtslag, 1987, p. 56, 71, 101)

$$\Psi_M = \begin{cases} 2\ln\left(\frac{1+x}{2}\right) + \ln\left(\frac{1+x^2}{2}\right) - 2\arctan(x) + \frac{\pi}{2}\,, & L < 0 \\ -\left[a\zeta + b\left(\zeta - \frac{c}{d}\right)\exp(-d\zeta) + \frac{bc}{d}\right]\,, & L > 0 \end{cases} \qquad \text{(D10)}$$

$$\Psi_H = \begin{cases} 2\ln\left(\frac{1+x^2}{2}\right)\,, & L < 0 \\ \Psi_M\,, & L > 0 \end{cases}$$

$$x = (1 - 16\zeta)^{1/4}$$

a=0.7, b=0.75, c=5, d=0.35

D1.6. Upper boundary conditions

$$\left.\frac{\partial \overline{u}}{\partial z}\right|_{\text{top}} = 0\,, \quad \left.\frac{\partial \overline{v}}{\partial z}\right|_{\text{top}} = 0\,, \quad \left.\frac{\partial \overline{\theta}}{\partial z}\right|_{\text{top}} = 0\,, \quad \left.\frac{\partial \overline{q}}{\partial z}\right|_{\text{top}} = 0\,, \quad \left.\frac{\partial \overline{\chi_\alpha}}{\partial z}\right|_{\text{top}} = 0. \qquad \text{(D11)}$$

D2. Second-order moments

D2.1. Initial conditions

At the starting time, second-order moments are zero.

ACPD
5, 11413–11487, 2005

D2.2. Lower boundary conditions

(References: Holtslag, 1987, p. 23–46)

Surface energy budget:

$$
\begin{aligned}
Q^{\star} &= H_{\mathrm{sfc}} + L_v E_{\mathrm{sfc}} + G_{\mathrm{soil}} \\
Q^{\star} &= (1 - \alpha_{\mathrm{sfc}}) K^{\downarrow} + L^{\uparrow} - L^{\downarrow} \\
Q^{\star} &= \frac{(1 - \alpha_{\mathrm{sfc}}) K^{\downarrow} + c_1 T_{\mathrm{scr}}^6 - \sigma T_{\mathrm{scr}}^4 + c_2 N_{\mathrm{cld}}}{1 + c_3} \\
K^{\downarrow} &= K^{\downarrow}_{\mathrm{clear}} (1 - b_1 N_{\mathrm{cld}}^{b_2}) \\
K^{\downarrow}_{\mathrm{clear}} &= a_1 \sin \Phi_{\mathrm{sun}} + a_2 \\
G_{\mathrm{soil}} &= c_G Q^{\star} \\
H_{\mathrm{sfc}} &= \frac{(1 - \alpha_{\mathrm{PM}}) + (\gamma_{\mathrm{PM}}/s)}{1 + (\gamma_{\mathrm{PM}}/s)} (Q^{\star} - G_{\mathrm{soil}}) - \beta_{\mathrm{PM}} \\
L_v E_{\mathrm{sfc}} &= \frac{\alpha_{\mathrm{PM}}}{1 + (\gamma_{\mathrm{PM}}/s)} (Q^{\star} - G_{\mathrm{soil}}) + \beta_{\mathrm{PM}} \\
\gamma_{\mathrm{PM}} &= \frac{c_p}{L_v} \\
s &= \frac{\partial q_s}{\partial T} \\
L_v &= (2.5 - 0.00236[T - 273.15]) \times 10^6 \,\mathrm{J\,kg^{-1}}
\end{aligned}
\tag{D12}
$$

T [°C]	-5	0	5	10	15	20	25	30	35
γ_{PM}/s	2.01	1.44	1.06	0.79	0.60	0.45	0.35	0.27	0.21

ACPD

5, 11413–11487, 2005

Friction velocity:

(a) For unstable conditions (References: Holtslag, 1987, p. 99–100, 106, 130)

$$L = -\frac{u_\star^3}{\kappa \frac{g}{\overline{T}(z_{k=1})}(\overline{w'\theta'})_{z_s}}$$

$$u_\star = \kappa \overline{U}(z_{k=1}) \left[\ln\left(\frac{z_p}{z_0}\right) - \Psi_M\left(\frac{z_p}{L}\right) + \Psi_M\left(\frac{z_0}{L}\right) \right]^{-1} \quad \text{(D13)}$$

Given the surface layer heat flux, the computation starts with $u_\star = \kappa \overline{U}(z_{k=1}) / \ln(z_p/z_0)$ for $\Psi_M = 0$ ($L = \infty$). In this way, an estimation of L is obtained. With this estimate, $u_\star$ is recalculated using improved Ψ_M and so on. The interation stops when $u_\star$ differs less than 5% from its anterior value.

(b) For stable conditions (References: Holtslag, 1987, p. 130)

$$L = \begin{cases} (L_n - L_0) + [L_n(L_n - 2L_0)]^{1/2}, & L_n \geq 2L_0 \\ \left(L_0 \frac{L_n}{2}\right)^{1/2}, & L_n < 2L_0 \end{cases}$$

$$L_0 = \frac{5 z_p}{\ln(\frac{z_p}{z_0})}$$

$$L_n = \frac{\kappa \overline{U}(z_{k=1})^2 \overline{T}(z_{k=1})}{2g\theta_\star \left[\ln \frac{z_p}{z_0}\right]^2} \quad \text{(D14)}$$

$$u_\star = \left(-\kappa \frac{g}{\overline{T}(z_{k=1})} (\overline{w'\theta'})_{z_s} L \right)^{1/3}$$

ACPD
5, 11413–11487, 2005

The computation starts with $\theta_\star \approx 0.09\,\mathrm{K}$ to obtain an estimation of L. With this estimate, $\theta_\star$ is recalculated using improved Ψ_H and so on. The interation stops when $\theta_\star$ differs less than 5% from its anterior value.

Surface Reynolds stresses (References: André et al., 1978):

$$\left(\overline{w'u'}\right)_{z_s} = -\left[\frac{\overline{u}(z_{\mathrm{k}=1})}{\overline{U}(z_{\mathrm{k}=1})}\right] u_\star^2\,, \quad \left(\overline{w'v'}\right)_{z_s} = -\left[\frac{\overline{v}(z_{\mathrm{k}=1})}{\overline{U}(z_{\mathrm{k}=1})}\right] u_\star^2\,, \quad \left(\overline{u'v'}\right)_{z_s} = 0\,, \tag{D15}$$

$$\left(\overline{u'u'}\right)_{z_s} = \begin{cases} 4u_\star^2 + 0.3w_\star^2\,, & \left(\overline{w'\theta'}\right)_{z_s} > 0 \\ 4u_\star^2\,, & \left(\overline{w'\theta'}\right)_{z_s} < 0 \end{cases},$$

$$\left(\overline{v'v'}\right)_{z_s} = \begin{cases} 1.75u_\star^2 + 0.3w_\star^2\,, & \left(\overline{w'\theta'}\right)_{z_s} > 0 \\ 1.75u_\star^2\,, & \left(\overline{w'\theta'}\right)_{z_s} < 0 \end{cases}, \tag{D16}$$

$$\left(\overline{w'w'}\right)_{z_s} = \begin{cases} \left[1.75 + 2(-\zeta)^{2/3}\right] u_\star^2\,, & \zeta < 0 \\ 1.75u_\star^2\,, & \zeta > 0 \end{cases}.$$

Surface layer components of the kinematic heat flux (References: André et al., 1978):

$$\left(\overline{u'\theta'}\right)_{z_s} = \left[\frac{\overline{u}(z_{\mathrm{k}=1})}{\overline{U}(z_{\mathrm{k}=1})}\right] \left(\overline{w'\theta'}\right)_{z_s} \times \begin{cases} -3.7(1-15\zeta)^{-1/4}(1-9\zeta)^{-1/2}\,, & \zeta < 0 \\ -3\,, & \zeta > 0 \end{cases},$$

$$\left(\overline{v'\theta'}\right)_{z_s} = \left[\frac{\overline{v}(z_{\mathrm{k}=1})}{\overline{U}(z_{\mathrm{k}=1})}\right] \left(\overline{w'\theta'}\right)_{z_s} \times \begin{cases} -3.7(1-15\zeta)^{-1/4}(1-9\zeta)^{-1/2}\,, & \zeta < 0 \\ -3\,, & \zeta > 0 \end{cases}, \tag{D17}$$

$$\left(\overline{w'\theta'}\right)_{z_s} = \frac{H_{\mathrm{sfc}}}{\rho_{\mathrm{air}} c_p}$$

Kinematic surface humidity flux:

$$\left(\overline{w'q'}\right)_{z_s} = \frac{E_{\mathrm{sfc}}}{\rho_{\mathrm{air}}} \tag{D18}$$

Variances, covariances of temperature and humidity (References: André et al., 1978):

$$(\overline{\theta'\theta'})_{z_s}\left[\frac{u_\star^2}{\left(\overline{w'\theta'}\right)_{z_s}^2}\right] = \left(\overline{q'q'}\right)_{z_s}\left[\frac{u_\star^2}{\left(\overline{w'q'}\right)_{z_s}^2}\right] = \left(\overline{\theta'q'}\right)_{z_s}\left[\frac{u_\star^2}{\left(\overline{w'\theta'}\right)_{z_s}\left(\overline{w'q'}\right)_{z_s}}\right] =$$

$$= \begin{cases} 4(1-8.3\zeta)^{-2/3}\,, & \zeta < 0 \\ 4\,, & \zeta > 0 \end{cases}. \tag{D19}$$

Convective tracer flux (dry deposition):

$$\left(\overline{w'\chi'_\alpha}\right)_{z_s} = -V_{\chi_\alpha}\overline{\chi}_\alpha(z_{\mathrm{k=1}}) \tag{D20}$$

Kinematic tracer flux (References: André et al., 1978):

$$\left(\overline{u'\chi'_\alpha}\right)_{z_s} = \left[\frac{\overline{u}(z_{\mathrm{k=1}})}{\overline{U}(z_{\mathrm{k=1}})}\right]\left(\overline{w'\chi'_\alpha}\right)_{z_s} \times \begin{cases} -3.7(1-15\zeta)^{-1/4}(1-9\zeta)^{-1/2}\,, & \zeta < 0 \\ -3\,, & \zeta > 0 \end{cases},$$

$$\left(\overline{v'\chi'_\alpha}\right)_{z_s} = \left[\frac{\overline{v}(z_{\mathrm{k=1}})}{\overline{U}(z_{\mathrm{k=1}})}\right]\left(\overline{w'\chi'_\alpha}\right)_{z_s} \times \begin{cases} -3.7(1-15\zeta)^{-1/4}(1-9\zeta)^{-1/2}\,, & \zeta < 0 \\ -3\,, & \zeta > 0 \end{cases} \tag{D21}$$

ACPD
5, 11413–11487, 2005

Variances, covariances of temperature, water vapor mixing ratio, and tracer concentration:

$$(\overline{\theta' \chi'_\alpha})_{z_s} \left[\frac{u_\star^2}{\left(\overline{w'\theta'}\right)_{z_s} \left(\overline{w'\chi'_\alpha}\right)_{z_s}} \right] = \begin{cases} 4(1-8.3\zeta)^{-2/3} \, , \, \zeta < 0 \\ 4 \, , \, \zeta > 0 \end{cases} ,$$

$$(\overline{q' \chi'_\alpha})_{z_s} \left[\frac{u_\star^2}{\left(\overline{w'q'}\right)_{z_s} \left(\overline{w'\chi'_\alpha}\right)_{z_s}} \right] = \begin{cases} 4(1-8.3\zeta)^{-2/3} \, , \, \zeta < 0 \\ 4 \, , \, \zeta > 0 \end{cases} , \quad \text{(D22)}$$

$$\left(\overline{\chi'_\alpha \chi'_\beta}\right)_{z_s} \left[\frac{u_\star^2}{\left(\overline{w'\chi'_\alpha}\right)_{z_s} \left(\overline{w'\chi'_\beta}\right)_{z_s}} \right] = \begin{cases} 4(1-8.3\zeta)^{-2/3} \, , \, \zeta < 0 \\ 4 \, , \, \zeta > 0 \end{cases}$$

D2.3. Upper boundary conditions

$$\left. \frac{\partial \overline{u'_i u'_j}}{\partial z} \right|_{\text{top}} (t) = 0 \, , \quad \left. \frac{\partial \overline{u'_i a'}}{\partial z} \right|_{\text{top}} (t) = 0 \, , \quad \left. \frac{\partial \overline{a' b'}}{\partial z} \right|_{\text{top}} (t) = 0 \quad \text{(D23)}$$

D3. Third-order moments

D3.1. Initial conditions

At the starting time, third-order moments are zero.

ACPD
5, 11413–11487, 2005

D3.2. Upper boundary conditions

$$\left.\frac{\partial \overline{u_i' u_j' w'}}{\partial z}\right|_{\text{top}} (t) = 0, \quad \left.\frac{\partial \overline{u_i' u_j' a'}}{\partial z}\right|_{\text{top}} (t) = 0, \quad \left.\frac{\partial \overline{u_i' a' b'}}{\partial z}\right|_{\text{top}} (t) = 0, \quad \left.\frac{\partial \overline{a' b' c'}}{\partial z}\right|_{\text{top}} (t) = 0. \quad \text{(D24)}$$

Appendix E

Numerics

E1. Adams-Bashforth time-differencing scheme

(References: Durran, 1999, p. 68, Table 2.1)

$$\begin{aligned} \frac{d\Psi}{dt} &= F(\Psi) \\ \Phi^n &= \Psi(n\,\Delta t) \\ \Phi^{n+1} &= \Phi^n + \frac{h}{12}\left[23\,F(\Phi^n) - 16\,F(\Phi^{n-1}) + 5\,F(\Phi^{n-2})\right] \end{aligned} \quad \text{(E1)}$$

E2. Vertical finite differencing scheme

(References: André et al., 1976a,b; Bougeault, 1985)

E2.1. Grid structure

Use of a staggered grid with first- and third-order correlations calculated at the same main levels and second-order ones at the intermediate levels

E2.2. Standard differencing scheme

$$\left.\frac{\partial \Phi}{\partial z}\right|_k = \frac{1}{2}\left(\tilde{D}_{up} + \tilde{D}_{down}\right)$$
$$\tilde{D}_{up} = \frac{\Phi_{k+1} - \Phi_k}{z_{k+1} - z_k} \quad \text{(E2)}$$
$$\tilde{D}_{down} = \frac{\Phi_k - \Phi_{k-1}}{z_k - z_{k-1}}$$

E2.3. Derivatives of mean-variables in third-order equations

Use of a "geometric approximation" of the derivatives of the mean variables in the third-order equations to avoid the appearance of negative values of variances just below the inversion

$$\left.\frac{\partial \Phi}{\partial z}\right|_k \approx 2\left|\tilde{D}_{up}\right|\left|\tilde{D}_{down}\right| \frac{\tilde{D}_{up} + \tilde{D}_{down}}{\left(\left|\tilde{D}_{up}\right| + \left|\tilde{D}_{down}\right|\right)^2} \quad \text{(E3)}$$

References

Aalto, P., Hämeri, K., Becker, E., Weber, R., Salm, J., Mäkelä, J. M., Hoell, C., O'Dowd, C. D., Karlsson, H., Hansson, H.-Ch., Väkevä, M., Koponen, I. K., Buzorius, G., and Kulmala, M.: Physical characterization of aerosol particles during nucleation events, Tellus, 53B, 344–358, 2001. 11415, 11419

Abdella, K. and McFarlane, N.: A new-second order turbulence closure scheme for the planetary boundary layer, J. Atmos. Sci., 54, 1850–1867, 1997. 11420

Abdella, K. and McFarlane, N.: Reply, J. Atmos. Sci., 56, 3482–3483, 1999. 11420

Abdella, K. and McFarlane, N.: Modelling boundary-layer clouds with a statistical cloud scheme and a second-order turbulence closure, Boundary-Layer Meteor., 98, 387–410, 2001. 11421

André, J. C., De Moor, G., Lacarrère, P., Therry, G., and Du Vachat, R.: Modeling the 24-hour evolution of the mean and turbulent structures of the planetary boundary layer, J. Atmos. Sci., 35, 1861–1883, 1978. 11421, 11441, 11450, 11470, 11471

André, J. C., De Moor, G., Lacarrère, P., Therry, G., and Du Vachat, R.: Turbulence approximation for inhomogeneous flows: Part I. The clipping approximation, J. Atmos. Sci., 33, 476–481, 1976a. 11421, 11450, 11473

André, J. C., De Moor, G., Lacarrère, P., Therry, G., and Du Vachat, R.: Turbulence approximation for inhomogeneous flows: Part II. The numerical simulation of a penetrative convection experiment, J. Atmos. Sci., 33, 481–491, 1976b. 11421, 11450, 11473

André, J. C., Lacarrère, P., and Traoré, K.: Pressure effects on triple correlations in turbulent convective flows, Turbulent Shear Flows, Springer Verlag, 3, 243–252, 1981. 11421, 11450

Andronache, C., Chameides, W. L., Davis, D. D., Anderson, B. E., Pueschel, R. F., Bandy, A. R., Thornton, D. C., Talbot, R. W., Kasibhatla, P., and Kiang, C. S.: Gas-to-particle conversion of tropospheric sulfur as estimated from observations in the western North Pacific during PEM-West B, J. Geophys. Res., 102, 28 511–28 538, 1997. 11415

Ansari, A. S. and Pandis, S. N.: Prediction of multicomponent inorganic atmospheric aerosol behavior, Atmos. Environ., 33, 745–757, 1999. 11428

Ayotte, K. W., Sullivan, P. P., Andrén, A., Doney, S. C., Holtslag, A. A. M., Large, W. G., McWilliams, J. C., Moeng, C.-H., Otte, M. J., Tribbia, J. J., and Wyngaard, J. C.: An evaluation of neutral and convective planetary boundary-layer parameterizations relative to large eddy simulations, Boundary-Layer Meteor., 79, 131–175, 1996. 11420

Berndt, T., Böge, O., Stratmann, F., Heintzenberg, J., and Kulmala, M.: Rapid formation of sulfuric acid particles at near-atmospheric conditions, Science, 307, 698–700, 2005. 11424, 11425

Bernhardt, K.: Zur Definition der turbulenzbedingten Austauschströme, insbesondere des Turbulenzwärmestroms, Z. Meteorol., 17, 95–108, 1964. 11430

Bernhardt, K.: Nochmals zur Definition des Turbulenzwärmestroms in der Wärmehaushaltsgleichung der Atmosphäre, Z. Meteorol., 23, 65–75, 1972. 11430

Bernhardt, K. and Piazena, H.: Zum Einfluß der turbulenzbedingten Dichteschwankungen auf die Bestimmung turbulenter Austauschströme in der Bodenschicht, Z. Meteorol., 38, 234–245, 1988. 11430

Bigg, E.: A mechanism for the formation of new particles in the atmosphere, Atmos. Res., 43, 129–137, 1997. 11414

Birmili, W.: On the formation and growth of new atmospheric particles in continental atmospheres, J. Aerosol Sci., 32, Suppl. 1, S321–S322, 2001. 11419

Birmili, W. and Wiedensohler, A.: New particle formation in the continental boundary layer: Meteorological and gas phase parameter influence, Geophys. Res. Lett., 27, 3325–3328, 2000. 11418, 11419

Birmili, W., Wiedensohler, A., Plass-Dülmer, C., and Berresheim, H.: Evolution of newly formed aerosol particles in the continental boundary layer: A case study including OH and H_2SO_4 measurements, Geophys. Res. Lett., 27, 2205–2208, 2000. 11416, 11419

Birmili, W., Berresheim, H., Plass-Dülmer, C., Elste, T., Gilge, S., Wiedensohler, A., and Uhrner, U.: The Hohenpeissenberg aerosol formation experiment (HAFEX): A long-term study including size-resolved aerosol, H_2SO_4, OH, and monoterpenes measurements, Atmos. Chem. Phys., 3, 361–376, 2003, SRef-ID: 1680-7324/acp/2003-3-361. 11416, 11419

Bohren, C. F. and Albrecht, B. A.: Atmospheric Thermodynamics, Oxford University Press, New York, 1998. 11414

Bougeault, P.: The diurnal cycle of the marine stratocumulus layer: A high-order model study, J. Atmos. Sci., 42, 2826–2843, 1985. 11473

Boy, M. and Kulmala, M.: Nucleation events in the continental boundary layer: Influence of physical and meteorological parameters, Atmos. Chem. Phys., 2, 1–16, 2002, SRef-ID: 1680-7324/acp/2002-2-1. 11415, 11419

Boy, M., Nilsson, D., and Kulmala, M.: BLMARC – A 1-dimensional model for the prediction of the aerosol evolution in the continental boundary layer, J. Aerosol Sci., EAC Abstracts, S821–S822, 2003. 11416

Boy, M., Petäjä, T., Dal Maso, M., Rannik, Ü., Rinne, J., Aalto, P., Laaksonen, A., Vaattovaara, P., Joutsensaari, J., Hoffmann, T., Warnke, J., Apostolaki, M., Stephanou, E. G., Tsapakis, M., Kouvarakis, A., Pio, C., Carvalho, A., Römpp, A., Moortgat, G., Spirig, C., Guenther, A., Greenberg, J., Ciccioli, P., and Kulmala, M.: Overview of the field measurement campaign in Hyytiälä, August 2001 in the framework of the EU project OSOA, Atmos. Chem. Phys., 4, 657–678, 2004, SRef-ID: 1680-7324/acp/2004-4-657. 11415, 11419

Boy, M., Rannik, Ü., Lehtinen, K. E. J., Tarvainen, V., Hakola, H., and Kulmala, M.: Nucleation events in the continental boundary layer: Long-term statistical analyzes of aerosol relevant characteristics, J. Geophys. Res., 108(D21), doi:10.1029/2003JD003838, 2003c. 11419,

11428
Brown, A. R.: Evaluation of parametrization schemes for the convective boundary layer using large-eddy simulation results, Boundary-Layer Meteor., 81, 167–200, 1996. 11420
Brown, A. R. and Grant, A. L. M.: Non-local mixing of momentum in the convective boundary layer, Boundary-Layer Meteor., 84, 1–22, 1997. 11420
Buzorius, G., Rannik, Ü., Nilsson, E. D., and Kulmala, M.: Vertical fluxes and micrometeorology during aerosol particle formation events, Tellus, Ser. B, 53, 394–405, 2001. 11415, 11419
Buzorius, G., Rannik, Ü., Aalto, P., Dal Maso, M., Nilsson, E. D., Lehtinen, K. E. J., and Kulmala, M.: On particle formation prediction in continental boreal forest using micrometeorological parameters, J. Geophys. Res., 108(D13), 4377, doi:10.1029/2002JD002850, 2003. 11415, 11419
Carlson, M. A. and Stull, R. B.: Subsidence in the nocturnal boundary layer, J. Clim. Appl. Met., 25, 1088–1099, 1986. 11422
Carson, D. J. and Richards, P. R. J.: Modelling surface turbulent fluxes in stable conditions, Boundary-Layer Meteor., 14, 67–81, 1978. 11467
Cheng, A., Xu, K.-M., and Golaz, J.-C.: The liquid water oscillation in modeling boundary layer cumuli with third-order turbulence closure models, J. Atmos. Sci., 61, 1621–1629, 2004. 11421
Clarke, A. D., Eisele, F. L., Kapustin, V. N., Moore, K., Tanner, D., Mauldin, L., Litchy, M., Lienert, B., Carroll, M. A., and Albercook, G.: Nucleation in the equatorial free troposphere: Favorable environments during PEM-Tropics, J. Geophys. Res., 104, 5735–5744, 1999. 11415
Clement, C. F. and Ford, I. J.: Gas-to-particle conversion in the atmosphere: I. Evidence from empirical atmospheric aerosols, Atmos. Environ., 33, 475–487, 1999a. 11416, 11419, 11428
Clement, C. F. and Ford, I. J.: Gas-to-particle conversion in the atmosphere: II. Analytical models of nucleation bursts, Atmos. Environ., 33, 489–499, 1999b. 11415, 11416, 11428, 11447
Clement, C. F., Pirjola, L., Dal Maso, M., Mäkelä, J. M., and Kulmala, M.: Analysis of particle formation bursts observed in Finland, J. Aerosol Sci., 32, 217–236, 2001. 11416, 11419
Coe, H., Williams, P. I., McFiggans, G., Gallagher, M. W., Beswick, K. M., Bower, K. N., and Choularton, T. W.: Behavior of ultrafine particles in continental and marine air masses at a rural site in the United Kingdom, J. Geophys. Res., 105, 26 891–26 905, 2000. 11414, 11419

Dal Maso, M., Kulmala, M., Lehtinen, K. E. J., Mäkelä, J. M., Aalto, P., and O'Dowd, C. D.: Condensation and coagulation sinks and formation of nucleation mode particles in coastal and boreal forest boundary layers, J. Geophys. Res., 107, doi:10.1029/2001JD001053, 2002. 11416

de Reus, M., Ström, J., Kulmala, M., Pirjola, L., Lelieveld, J., Schiller, C., and Zöger, M.: Airborne aerosol measurements in the tropopause region and the dependence of new particle formation on preexisting particle number concentration, J. Geophys. Res., 103, 31 255–31 263, 1998. 11424

de Reus, M., Ström, J., Hoor, P., Lelieveld, J., and Schiller, C.: Particle production in the lowermost stratosphere by convective lifting of the tropopause, J. Geophys. Res., 104, 23 935–23 940, 1999. 11415

Donaldson, C. duP.: Construction of a dynamic model of the production of atmospheric turbulence and the dispersal of atmospheric pollutants, Workshop on Micrometeorology, edited by: Haugen, D. A., American Meteorological Society, Boston, 313–392, 1973. 11418

Durran, D. R.: Numerical Methods for Wave Equations in Geophysical Fluid Dynamics, Springer-Verlag New York Berlin Heidelberg, 1999. 11473

Dyer, A. J. and Hicks, B. B.: Flux-gradient relationships in the constant flux layer, Quart. J. Roy. Meteor. Soc., 96, 715–721, 1970. 11465

Easter, R. C. and Peters, L. K.: Binary homogeneous nucleation: Temperature and relative humidity fluctuations, nonlinearity, and aspects of new particle production in the atmosphere, J. Appl. Meteor., 33, 775–784, 1994. 11415, 11429

Ebert, E. E., Schumann, U., and Stull, R. B.: Nonlocal turbulent mixing in the convective boundary layer evaluated from large-eddy simulation, J. Atmos. Sci., 46, 2178–2207, 1989. 11420

Elperin, T., Kleeorin, N., and Rogachevskii, I.: Mechanism of formation of aerosol and gaseous inhomogeneities in the turbulent atmosphere, Atmos. Res., 53, 117–129, 2000. 11415

Ferrero, E. and Racca, M.: The role of the nonlocal transport in modeling the shear-driven atmospheric boundary layer, J. Atmos. Sci., 61, 1434–1445, 2004. 11420, 11421

Foken, T.: Die universelle Funktion nach Skeib – Grundlage für Maßstabsbetrachtungen in der atmosphärischen Bodenschicht, Z. Meteorol., 39, 112–113, 1989. 11430

Frech, M. and Mahrt, L.: A two-scale mixing formulation for the atmospheric boundary layer, Boundary-Layer Meteor., 73, 91–104, 1995. 11420

Galmarini, S., Vilà-Guerau De Arellano, J., and Duynkerke, P. G.: Scaling the turbulent transport of chemical compounds in the surface layer under neutral and stratified conditions, Quart. J.

Roy. Meteor. Soc., 123, 223–242, 1997. 11421
Gaydos, T. M. and Stanier, C. O.: Modeling of in situ ultrafine atmospheric particle formation in the eastern United States, J. Geophys. Res., 110, doi:10.1029/2004JD004683, 2005. 11416, 11417, 11419, 11428
Held, A., Nowak, A., Birmili, W., Wiedensohler, A., Forkel, R., and Klemm, O.: Observations of particle formation and growth in a mountainous forest region in central europe, J. Geophys. Res., 109, doi:10.1029/2004JD005346, 2004. 11415, 11418, 11419, 11428
Hellmuth, O. and Helmert, J.: Parameterization of turbulence-enhanced nucleation in large scale models: Conceptual study, in: Air Pollution Modeling and Its Application XV, edited by: Borrego, C. and Schayes, G., Kluwer Academic/ Plenum Publishers, New York, pp. 295–304, 2002. 11415, 11429
Hermann, M., Heintzenberg, J., Wiedensohler, A., Zahn, A., Heinrich, G., and Brenninkmeijer, C. A. M.: Meridional distributions of aerosol particle number concentrations in the upper and lower stratosphere obtained by Civil Aircraft for Regular Investigation of the Atmosphere Based on an Instrument Container (CARIBIC) flights, J. Geophys. Res., 108, doi:10.1029/2001JD001077, 2003. 11415
Holtslag, A. A. M.: Surface fluxes and boundary layer scaling, Scientific reports WR-nr 87-2, Koninklijk Nederlands Meteorologisch Instituut, 1987. 11422, 11466, 11467, 11468, 11469
Holtslag, A. A. M. and Moeng, C.-H.: Eddy diffusivity and countergradient transport in the convective atmospheric boundary layer, J. Atmos. Sci., 48, 1690–1698, 1991. 11420
Housiadas, C., Drossinos, Y., and Lazaridis, M. L.: Effect of small-scale turbulent fluctuations on rates of particle formation, J. Aerosol Sci., 35, 545–559, 2004. 11415
IPCC: IPCC Third Assessment Report, The Scientific Basis, Tech. Rep., Intergovernmental Panel on Climate Change, 2001. 11421
Jaecker-Voirol, A. and Mirabel, A. P.: Nucleation rate in a binary mixture of sulfuric acid and water vapor, J. Phys. Chem., 92, 3518–3521, 1988. 11426
Jaecker-Voirol, A. and Mirabel, A. P.: Heteromolecular nucleation in the sulfuric acid-water system, Atmos. Environ., 23, 2053–2057, 1989. 11426
Jaecker-Voirol, A., Mirabel, A. P., and Reiss, H.: Hydrates in supersaturated binary sulfuric acid-water vapor: A re-examination, J. Chem. Phys., 87, 4849–4852, 1987. 11426
Jaenisch, V., Stratman, F., Nilsson, D., and Austin, P. H.: Influence of turbulent mixing processes on new particle formation, J. Aerosol Sci., 29, S1063–S1064, 1998a. 11415
Jaenisch, V., Stratman, F., and Wilck, M.: Particle nucleation and condensational growth during

turbulent mixing processes, J. Aerosol Sci., 29, S1161–S1162, 1998b. 11415
Katoshevski, D., Nenes, A., and Seinfeld, J. H.: A study of processes that govern the maintenance of aerosols in the marine boundary layer, J. Aerosol Sci., 30, 503–532, 1999. 11416
Kerminen, V.-K. and Kulmala, M.: Analytical formulae connecting the "real" and the "apparent" nucleation rate and the nuclei number concentration for atmospheric nucleation events, J. Aerosol Sci., 33, 609–622, 2002. 11416, 11426
Kerminen, V.-K. and Wexler, A. S.: Growth behavior of the marine submicron boundary layer aerosol, J. Geophys. Res., 102, 18 813–18 825, 1997. 11416
Khosrawi, F. and Konopka, P.: Enhanced particle formation and growth due to mixing processes in the tropopause region, Atmos. Environ., 37, 903–910, 2003. 11415
Komppula, M., Dal Maso, M., Lihavainen, H., Kulmala, M., and Viisanen, Y.: Comparison of new particle formation events at two locations in Northern Finland, J. Aerosol Sci., EAC Abstracts, S743–S744, 2003. 11417
Korhonen, H., Lehtinen, K. E. J., and Kulmala, M.: Multicomponent aerosol dynamics model UHMA: Model development and validation, Atmos. Chem. Phys., 4, 471–506, 2004, SRef-ID: 1680-7324/acp/2004-4-471. 11416
Korhonen, P., Kulmala, M., Laaksonen, A., Viisanen, Y., McGraw, R., and Seinfeld, J.: Ternary nucleation of H_2SO_4, NH_3, and H_2O in the atmosphere, J. Geophys. Res., 104, 26 349–26 353, 1999. 11424
Krejci, R., Ström, J., de Reus, M., Hoor, P., Williams, J., Fischer, H., and Hansson, H.-C.: Evolution of aerosol properties over the rain forest in Surinam, South America, observed from aircraft during the LBA-CLAIRE 98 experiment, J. Geophys. Res., 108, doi:10.1029/2001JD001375, 2003. 11428
Krishnamurti, T. N. and Bounoua, L. (Eds.): An Introduction to Numerical Weather Prediction Techniques, CRC Press LLC Boca Raton, 1996. 11422
Kulmala, M. and Laaksonen, A.: Binary nucleation of water-sulfuric acid system: Comparison of classical theories with different H_2SO_4 saturation vapor pressure, J. Chem. Phys., 93, 696–701, 1990. 11426
Kulmala, M., Kerminen, V.-M., and Laaksonen, A.: Simulations on the effect of sulphuric acid formation on atmospheric aerosol concentrations, Atmos. Environ., 29, 377–382, 1995. 11416, 11423
Kulmala, M., Laaksonen, A., and Pirjola, L.: Parameterizations for sulfuric acid/ water nucleation rates, J. Geophys. Res., 103(D7), 8301–8307, 1998. 11424, 11426

Kulmala, M., Dal Maso, M., Mäkelä, J. M., Pirjola, L., Väkevä, M., Aalto, P., Miikkulainen, P., Hämeri, K., and O'Dowd, C. D.: On the formation, growth and composition of nucleation mode particles, Tellus, 53B, 479–490, 2001. 11419

Kulmala, M., Napari, I., Merikanto, J., Vehkamäki, H., Laakso, L., Lehtinen, K. E. J., Noppel, M., and Laaksonen, A.: Homogeneous and ion induced nucleation: Kinetic and thermodynamic nucleation regimes, J. Aerosol Sci., EAC Abstracts, S1393–S1394, 2003. 11423, 11424

Kulmala, M., Vehkamäki, H., Petäjä, T., Dal Maso, M., Lauri, A., Kerminen, V.-M., Birmili, W., and McMurry, P. H.: Formation and growth rates of ultrafine atmospheric particles: A review of observations, J. Aerosol Sci., 35, 143–176, 2004. 11414, 11419

Laaksonen, A. and Kulmala, M.: Homogeneous heteromolecular nucleation of sulphuric acid and water vapours in stratospheric conditions: A theoretical study of the effect of hydrate interaction, J. Aerosol Sci., 22, 779–787, 1991. 11426

Larson, V. E.: Prognostic equations for cloud fraction and liquid water, and their relation to filtered density functions, J. Atmos. Sci., 61, 338–351, 2004. 11421

Lauros, J., Nilsson, E. D., Vehkamäki, H., and Kulmala, M.: Effect of variability in temperature and humidity on binary water-sulfuric acid nucleation rate, Proceedings of ICNAA 2004, Kyoto, 2004. 11415, 11429

Lesniewski, T. and Friedlander, S. K.: The effect of turbulence on rates of particle formation by homogeneous nucleation, Aerosol Sci. Tech., 23, 174–182, 1995. 11415

Lewellen, D. C. and Lewellen, W. S.: Buoyancy flux modeling for cloudy boundary layers, J. Atmos. Sci., 61, 1147–1160, 2004. 11421

Liu, X., Hegg, D. A., and Stoelinga, M. T.: Numerical simulation of new particle formation over northwest Atlantic using MM5 mesoscale model coupled with sulfur chemistry, J. Geophys. Res., 106, 9697–9715, 2001. 11428, 11447, 11449, 11462

Lovejoy, E. R., Curtius, J., and Froyd, K. D.: Atmospheric ion-induced nucleation of sulphuric acid and water, J. Geophys. Res., 109, doi:10.1029/2003JD004460, 2004. 11423, 11425

Marti, J. J., Weber, R. J., McMurry, P. H., Eisele, F., Tanner, D., and Jefferson, A.: New particle formation at a remote continental site: Assessing the contribution of SO_2 and organic precursors, J. Geophys. Res., 102, 6331–6339, 1997. 11424

Mironov, D. V., Gryanik, V. M., Lykossov, V. N., and Zilitinkevich, S. S.: Comments on "A new second-order turbulence closure scheme for the planetary boundary layer", J. Atmos. Sci., 56, 3478–3481, 1999. 11420

Moeng, C.-H. and Randall, D. A.: Problems in simulating the stratocumulus-topped boundary

layer with a third-order closure model, J. Atmos. Sci., 41, 1588–1600, 1984. 11422, 11423
Müller, K.: A 3 year study of the aerosol in northwest Saxony (Germany), Atmos. Environ., 33, 1679–1685, 1999. 11424
Napari, I., Noppel, M., Vehkamäki, H., and Kulmala, M.: An improved model for ternary nucleation of sulfuric acid – ammonia – water, J. Chem. Phys., 116, 4221–4227, 2002a. 11425, 11427
Napari, I., Noppel, M., Vehkamäki, H., and Kulmala, M.: Parametrization of ternary nucleation rates for H_2SO_4-NH_3-H_2O vapors, J. Geophys. Res., 107, doi:10.1029/2002JD002132, 2002b. 11427
Nenes, A., Pilinis, C., and Pandis, S. N.: ISORROPIA V1.5 Reference Manual, University of Miami, Carnegie Mellon University, 2000. 11428
Nilsson, E. D. and Kulmala, M.: The potential for atmospheric mixing processes to enhance the binary nucleation rate, J. Geophys. Res., 103, 1381–1389, 1998. 11414
Nilsson, E. D., Pirjola, L., and Kulmala, M.: The effect of atmospheric waves on aerosol nucleation and size distribution, J. Geophys. Res., 105, 19 917–19 926, 2000a. 11414
Nilsson, E. D., Rannik, Ü., Paatero, J., Boy, M., O'Dowd, C. D., Buzorius, G., Laakso, L., and Kulmala, M.: Effects of synoptic weather and boundary layer dynamics on aerosol formation in the continental boundary layer, J. Aerosol Sci., 31, S600–S602, 2000b. 11415
Nilsson, E. D., Paatero, J., and Boy, M.: Effects of air masses and synoptic weather on aerosol formation in the continental boundary layer, Tellus, 53B, 462–478, 2001a. 11415, 11416, 11419
Nilsson, E. D., Rannik, Ü., Kulmala, M., and O'Dowd, C. D.: Effects of continental boundary layer evolution, convection, turbulence and entrainment, on aerosol formation, Tellus, 53B, 441–461, 2001b. 11415
Noppel, M., Vehkamäki, H., and Kulmala, M.: An improved model for hydrate formation in sulfuric acid-water nucleation, J. Chem. Phys., 116, 218–228, 2002. 11426
Nyeki, S., Kalberer, M., Lugauer, M., Weingartner, E., Petzold, A., Schröder, F., Colbeck, I., and Baltensperger, U.: Condensation nuclei (CN) and ultrafine CN in the free troposphere to 12 km: A case study over the Jungfraujoch high-alpine research station, Geophys. Res. Lett., 26, 2195–2198, 1999. 11414
O'Dowd, C. D., Hämeri, K., Mäkelä, J. M., Pirjola, L., Kulmala, M., Jennings, S. G., Berresheim, H., Hansson, H., de Leeuw, G., Kunz, G. J., Allen, A. G., Hewitt, C. N., Jackson, A., Viisanen, Y., and Hoffmann, T.: A dedicated study of new particle formation and fate in the coastal

environment (PARFORCE): Overview of objectives and achievements, J. Geophys. Res., 107, doi:10.1029/2001JD000555, 2002. 11414
O'Dowd, C. D., Aalto, P. P., Yoon, Y. J., and Hämeri, K.: The use of the pulse height analyser ultrafine condensation particle counter (PHA-UCPC) technique applied to sizing of nucleation mode particles of differing chemical composition, J. Aerosol Sci., 35, 205–216, 2004. 11419
Pandis, S. N., Wexler, A. S., and Seinfeld, J. H.: Dynamics of tropospheric aerosols, J. Phys. Chem., 99, 9646–9659, 1995. 11424
Paulson, C. A.: The mathematical representation of wind speed and temperature profiles in the unstable atmospheric surface layer, J. Appl. Meteorol., 9, 856–861, 1970. 11467
Pirjola, L.: Effects of the increased UV radiation and biogenic VOC emissions on ultrafine sulphate aerosol formation, J. Aerosol Sci., 30, 355–367, 1999. 11416
Pirjola, L. and Kulmala, M.: Modelling the formation of H_2SO_4-H_2O particles in rural, urban and marine marine conditions, Atmos. Res., 46, 321–347, 1998. 11416, 11423
Pirjola, L., Kulmala, M., Wilck, M., Bischoff, A., Stratmann, F., and Otto, E.: Formation of sulphuric acid aerosols and cloud condensation nuclei: An expression for significant nucleation and model comparison, J. Aerosol Sci., 30, 1079–1094, 1999. 11423, 11444
Pirjola, L., O'Dowd, C. D., Brooks, I. M., and Kulmala, M.: Can new particle formation occur in the clean marine boundary layer?, J. Geophys. Res., 105, 26 531–26 546, 2000. 11414
Pirjola, L., Tsyro, S., Tarrason, L., and Kulmala, M.: A monodisperse aerosol dynamics module, a promising candidate for use in long-range transport models: Box model tests, J. Geophys. Res., 108, doi:10.1029/2002JD002867, 2003. 11423
Plauskaite, K., Gaman, A. I., Aalto, P., Mordas, G., Ulevicius, V., Lehtinen, K. E. J., and Kulmala, M.: Characterisation of nucleation events at Preila and Hyytiälä stations, J. Aerosol Sci., EAC Abstracts, S731–S732, 2003. 11416
Pleim, J. E. and Chang, J. S.: A non-local closure model for vertical mixing in the convective boundary layer, Atmos. Environ., 26A, 965–981, 1992. 11420
Raes, F. and Janssens, A.: Ion-induced aerosol formation in a H_2O-H_2SO_4 system – II. Numerical calculations and conclusions, J. Aerosol Sci., 17, 715–722, 1986. 11416
Russell, L. M., Lenschow, D. H., Laursen, K. K., Krummel, P. B., Siems, S. T., Bandy, A. R., Thornton, D. C., and Bates, T. S.: Bidirectional mixing in an ACE 1 marine boundary layer overlain by a second turbulent layer, J. Geophys. Res., 103, 16 411–16 432, 1998. 11414
Schröder, F. and Ström, J.: Aircraft measurements of submicrometer aerosol particles (>7 nm) in the midlatitude free troposphere and tropopause region, Atmos. Res., 44, 333–356, 1997.

11415
Schröder, F., Kärcher, B., Fiebig, M., and Petzold, A.: Aerosol states in the free troposphere at northern midlatitudes, J. Geophys. Res., 107, doi:10.1029/2000JD000194, 2002. 11415
Seinfeld, J. H. and Pandis, S. N.: Atmospheric Chemistry and Physics, From Air Pollution to Climate Change, John Wiley & Sons, Inc., 1998. 11426, 11427, 11428, 11447, 11448
Shaw, B. D.: Asymptotic evaluation of probability density functions for mean aerosol particle formation rates by homogeneous nucleation in turbulent gas jets, J. Aerosol Sci., 35, 177–184, 2004. 11415, 11429
Siebert, H., Stratmann, F., and Wehner, B.: First observations of increased ultrafine particle number concentrations near the inversion of a continental planetary boundary layer and its relation to ground-based measurements, Geophys. Res. Lett., 31, doi:10.1029/2003GL019086, 2004. 11415, 11416, 11419
Siebesma, A. P. and Holtslag, A. A. M.: Model impacts of entrainment and detrainment rates in shallow cumulus convection, J. Atmos. Sci., 53, 2354–2364, 1996. 11420
Sorbjan, Z.: Numerical study of penetrative and 'solid lid' nonpenetrative convective boundary layer, J. Atmos. Sci., 53, 101–112, 1996. 11420
Stanier, C. O., Khlystov, A. Y., Zhang, Q., Jimenez, J. L., Caragaratna, M., Worsnop, D., and Pandis, S. N.: Examining sulfuric acid nucleation events in the Northeast United States, J. Aerosol Sci., EAC Abstracts, S1343–S1344, 2003. 11418, 11424
Stauffer, D.: Kinetic theory of two-component ("heteromolecular") nucleation and condensation, J. Aerosol Sci., 7, 319–333, 1976. 11426
Steinbrecher, R. and BEWA2000-Team: Regional biogenic emissions of reactive volatile organic compounds (BVOC) from forests: Process studies, modelling and validation experiments (BEWA2000), AFO2000 Newsletter 8, GSF-Forschungszentrum für Umwelt und Gesundheit, GmbH, GSF-Forschungszentrum für Umwelt und Gesundheit, GmbH, Projektträger in der GSF, Kühbachstr. 11, D-81543 München, unpublished manuscript, available at: http://imk-ifu.fzk.de/bewa2000/openMaterial/AFO_Newsl_Beitrag_steinbrecher_11.pdf, 2004. 11419
Stratmann, F., Siebert, H., Spindler, G., Wehner, B., Althausen, D., Heintzenberg, J., Hellmuth, O., Rinke, R., Schmieder, U., Seidel, C., Tuch, T., Uhrner, U., Wiedensohler, A., Wandinger, U., Wendisch, M., Schell, D., and Stohl, A.: New-particle formation events in a continental boundary layer: First results from the SATURN experiment, Atmos. Chem. Phys., 3, 1445–1459, 2003,

SRef-ID: 1680-7324/acp/2003-3-1445. 11415, 11416, 11419
Stull, R. B.: An Introduction to Boundary Layer Meteorology, Kluwer Academic Publishers, Dordrecht/Boston/London, 1997. 11417, 11418, 11438, 11453
Sullivan, P. P., Moeng, C.-H., Stevens, B., Lenschow, D. H., and Mayor, S. D.: Structure of the entrainment zone capping the convective atmospheric boundary layer, J. Atmos. Sci., 55, 3042–3064, 1998. 11420
Thuburn, J. and Tan, D. G. H.: A parameterization of mixdown time for atmospheric chemicals, J. Geophys. Res., 102, 13 037–13 049, 1997. 11421
Uhrner, U., Birmili, W., Stratmann, F., Wilck, M., Ackermann, I., and Berresheim, H.: Particle formation at a continental background site: Comparision of model results with observations, Atmos. Chem. Phys., 3, 347–359, 2003,
SRef-ID: 1680-7324/acp/2003-3-347. 11415, 11416
van Dop, H.: Discussion: The parameterization of the vertical dispersion of a scalar in the atmospheric boundary layer, Atmos. Environ., 32, 257–258, 1998. 11430
Vana, M., Kulmala, M., Dal Maso, M., Hõrrak, U., and Tamm, E.: Comparative study of nucleation mode aerosol particles and intermediate air ions formation events at three sites, J. Geophys. Res., 109, doi:10.1029/2003JD004413, 2004. 11417
Vehkamäki, H., Kulmala, M., Napari, I., Lehtinen, K. E. J., Timmreck, C., Noppel, M., and Laaksonen, A.: An improved parameterization for sulfuric acid – water nucleation rates for tropospheric and stratospheric conditions, J. Geophys. Res., 107, doi:10.1029/2002JD002184, 2002. 11425
Venkatram, A.: The parameterization of the vertical dispersion of a scalar in the atmospheric boundary layer, Atmos. Environ., 27A, 1963–1966, 1993. 11430
Verver, G. H. I., van Dop, H., and Holtslag, A. A. M.: Turbulent mixing of reactive gases in the convective boundary layer, Boundary-Layer Meteor., 85, 197–222, 1997. 11421
Vinuesa, J.-F. and Vilá-Guerau de Arellano, J.: Introducing effective reaction rates to account for the inefficient mixing of the convective boundary layer, Atmos. Environ., 39, 445–461, 2005. 11421
Weber, R. J., Marti, J. J., McMurry, P. H., Eisele, F. L., Tanner, D. J., and Jefferson, A.: Measured atmospheric new particle formation rates: Implications for nucleation mechanisms, Chem. Eng. Comm., 151, 53–64, 1996. 11424
Wehner, B. and Wiedensohler, A.: Long term measurements of submicrometer urban aerosols: Statistical analysis for correlations with meteorological conditions and trace gases, Atmos.

Chem. Phys., 3, 867–879, 2003,
SRef-ID: 1680-7324/acp/2003-3-867. 11416
Wehner, B., Schmieder, U., Siebert, H., Stratmann, F., Spindler, G., Tuch, T., and Wiedensohler, A.: Horizontal variability of new particle formation during SATURN, J. Aerosol Sci., EAC Abstracts, S725–S726, 2003. 11416
Whitby, E. R. and McMurry, P. H.: Modal aerosol dynamics modeling, Aerosol Sci. Technol., 27, 673–688, 1997. 11416
Wichmann, M. and Schaller, E.: Comments on "Problems in simulating the stratocumulus-topped boundary layer with a third-order closure model", J. Atmos. Sci., 42, 1559–1561, 1985. 11421, 11422
Wichmann, M. and Schaller, E.: On the determination of the closure parameters in high-order closure models, Boundary-Layer Meteor., 37, 323–341, 1986. 11421
Wilck, M.: Modal modelling of multicomponent aerosols, PhD dissertation, Universität Leipzig, Leipzig, 1998. 11416
Wilck, M. and Stratmann, F.: A 2-D multicomponent modal aerosol model and its application to laminar flow reactors, J. Aerosol Sci., 28, 959–972, 1997. 11416
Yu, F.: Nucleation rate of particles in the lower atmosphere: Estimated time needed to reach pseudo-steady state and sensitivity to H_2SO_4 gas concentration, Geophys. Res. Lett., 30, 1526, doi:10.1029/2003GL017084, 2003. 11424
Yu, F. and Turco, R. P.: From molecular clusters to nanoparticles: role of ambient ionization in tropospheric aerosol formation, J. Geophys. Res., 106, 4797–4814, 2001. 11425, 11426
Zhang, L., Gong, S., Padro, J., and Barrie, L.: A size-segregated particle dry deposition scheme for an atmospheric aerosol module, Atmos. Environ., 35, 549–560, 2001. 11428
Zilitinkevich, S. S., Gryanik, V. M., Lykossov, V. N., and Mironov, D. V.: Third-order transport and nonlocal turbulence closures for convective boundary layers, J. Atmos. Sci., 56, 3463–3477, 1999. 11421

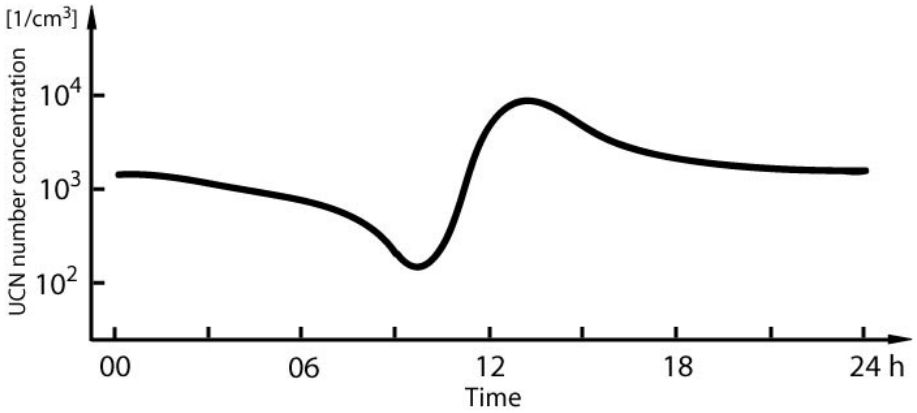

Fig. 1. Typical UCN evolution in the CSL during a NPF burst.

ACPD
5, 11413–11487, 2005